Università
degli Studi
di Padova

Dipartimento
di Ingegneria
dell'Informazione

Control of HVAC Systems via Implicit and Explicit MPC: an Experimental Case Study

Laureando

Luca Fabietti

Relatore

Prof. Alessandro Beghi

Correlatore

Prof. Karl H. Johansson

Dipartimento di
Ingegneria
dell'Informazione

Anno 2014

Abstract

Buildings are among the largest consumers of energy in the world. A significant part of this energy can be attributed to Heating, Ventilation and Air Conditioning (HVAC) systems, which play an important role in maintaining acceptable thermal and air quality conditions in common building. For this reason, improving energy efficiency in buildings is today a primary objective for the building industry, as well as for the society in general.

However, in order to successfully control buildings, control systems must continuously adapt the operation of the building to various uncertainties (external air temperature, occupants' activities, etc.) while making sure that energy efficiency does not compromise occupant's comfort and well-being. Several promising approaches have been proposed; among them, Model Predictive Control has received particular attention, since it can naturally achieve systematic integration of several factors, such as weather forecasts, occupancy predictions, comfort ranges and actuation constraints. This advanced technique has been shown to bring significant improvements in energy savings.

Model Predictive Control employs a model of the system and solves an on-line optimization problem to obtain optimal control inputs. The on-line computation, as well as the modelling effort, can lead to difficulties in the practical integration into a building management system.
To cope with this problem, another possibility is to obtain off-line the optimal control profile as a piecewise affine and continuous function of the initial state. By doing so, the computation associated with Model Predictive Control becomes a simple function evaluation, which can be performed efficiently on a simple and cheap hardware.

In this thesis, an implicit and an explicit formulation of Model Predictive Control for HVAC systems are developed and compared, showing the practical advantages of the explicit formulation.

Acknowledgements

The name that holds the cover of this thesis is just one, but behind it there are many of people who have played a key role in helping me to get where I am now and to be the person I am. It is difficult to express in few words how grateful I am. You have allowed me to grow and improve day after day, everyone teaching me something that I will carry with me for the rest of my life.

First of all I would like to thank Prof. Beghi Alessandro and Prof. Karl Henrik Johansson for having given me the opportunity to spend a beautiful period in Stockholm. It has been one of the of the richest moments of excitement and news of my entire life, a continuous process of growth and improvement which lasted six months.

Thanks to the HVAC research group Alessandra, Marco, Damiano and Giorgio for having been always kind, caring and helpful towards me. Thanks for the advices, for your patience, for your continuous support. For six months I felt as if I was at home guarded by four older brothers.

Thanks to my family for all the sacrifices and things you have done, that you are doing, and that I know you will always do for me. Thanks to my dad, Fabio, for being so careful not to let me lack anything that I needed; to my mum, Adriana, to be always present when I needed you; to my little sisters, Barbara and Claudia for making me proud of you everyday. Thanks to my aunts and uncles, Elisabetta, Chiara, Guido, Cristiano you have guided me throughout my whole life and I know that I could not wish for a better family than ours.

Thanks to Keko, Rocco, Milo, Volpe, Papa, Alessandra, Simona, Giulia, Olga, Erika and Max for always having been real and honest friends. It is really difficult to find people that you know you can trust and share everything with. I am really lucky to have you.

Thanks to Charlotte, Manuel, Sofia, Paul, Albane, Chris, Dario, Jennifer and Fabio for making me feel like part of a family all the time during my period here. The time I spent with you was really great and I know that I will miss you all.

Thanks to my corridor mates for being so nice and for making me feel so comfortable in my room. Especially I wanted to thank Johan for all the time we spent together.

Thanks to Martina for having been my girlfriend for 7 years. I owe you a lot and I hope that in the future it would be possible to create a new friendship between us.

Thanks to Veces, Fabrice, Marie, Paul, Cyrille, Rui and Jordi for the six months we spent together in the master thesis room sharing all the problems and making our path more enjoyable.

Thanks to all the people which helped me becoming an engineer, all the friends at university, all my football team mates, all those who entered in my life even just for a while. I know that I will bring a piece of you with me forever.

I leave at the end a very special thanks for my grandparents. You have been like parents for me in all my life, you were always ready to help me and my family in every occasion. I am sure that a lot of the person I am is thanks to you and your precious teaching. I love you more than I often show.

Contents

List of Tables

List of Figures

1

Introduction

A major issue of our times is that of energy consumption, due to both the depletion of fossil fuel energy sources and the environmental impact that comes from the associated energy waste. Within Europe, the total energy consumption is increasing at a rate of 1.5% per year, due to several factors like economic growth, expansion of building sector, and spread of building services. As a direct consequence, the scientific community worldwide is making many efforts to improve the overall energy efficiency of mankind activities. In particular, European energy consumption presents the following energy distribution: 34.6% in transport, 24.6% in management of households, 27.9% in industry and 14.9% in commercial and others [1]. Summarizing, these statistics show how buildings, both residential and commercial, account for a total amount of approximatively 40% of the total energy consumption.

Given these figures, it is no surprising that academic and industrial research groups have been working on achieving improvements in energy savings for buildings. A special attention is then reserved to the so-called Heating, Venting and Air Conditioning (HVAC) systems, i.e., the set of equipments that condition and distribute the indoor air of a building, and that are dedicated to the maintenance of its quality. In this context, it is worth knowing that HVAC

systems account for 50% of buildings energy consumption and approximately 20% of total consumption [1].

Moreover, it is well known that HVAC systems use more energy than expected or desired, and it has been estimated that there is a potential energy savings that ranges between 5% and 30% [2]. Out of this need the concept of *intelligent buildings* is becoming more common nowadays. The current trend is indeed to equip buildings with instruments and sensors that collect data that are then used by complex control techniques to improve energetic performances while maintaining comfort levels.

Model Predictive Control has gained a lot of attention over the last years, especially for the control of buildings [3]. This is due to its ability to use a model-based control technique that integrates a mathematical representation of the building with the most important factors which affect the building dynamics. For instance with this scheme it is possible to integrate physical constraints on actuators, forecasts of disturbances acting on the building, and predictions on future weather and occupancy conditions.

But while all these properties make MPC extremely powerful and attractive when it comes to building control, at the same time designing a proper controller is a challenging task. Indeed, it requires an extensive knowledge of the physical properties of the building, as well as data processing, and computational efforts.

1.1 Review of technologies and control techniques in HVAC systems

This section presents the current state of the art on the control of HVACs systems. In particular, we provide a description of the technologies and methodologies currently applied on modern HVACs system.

We then start clarifying what is actually an HVAC system: an HVAC system is a set of mechanical devices that are designed and coupled to condition and distribute the air inside a building, so that this air satisfies certain quality conditions (for an indoor environment). This quality control is usually achieved by conditioning the temperature, humidity, cleanliness and motion of the air. A basic system often includes an outside-air intake, a chiller pre-heater, a dehumidifier, some fans, some ducts, air outlets, and air terminals.

General technologies used in HVAC systems

As mentioned in the introduction, advanced control techniques also require knowledge, under the form of data describing the current status of the indoor environment. To this aim, a common practice is to provide HVACs systems with dedicated measurement systems, like WSNs. The aim is to monitor physical or environment conditions like temperature, CO_2, humidity, and occupancy levels.

In particular, WSNs are currently widely used because they are cost-effective: indeed they are easy to retrofit in existing buildings, and besides they require minimal maintenance and supervision. We incidentally notice that another important aspect to be considered is that of privacy: since the main aim of an HVAC system is to assure comfort conditions to the users, it is crucial to use sensors which do not affect users' behaviors and do not raise privacy concerns. For all these reasons, WSNs represent an interesting choice.

The most used sensors among those that are currently exploited can be summarized as:

- temperature, humidity, light and CO_2 sensors;
- acoustic sensors (also microphones);
- Passive Infrared (PIR) sensors (for motion detection or people counting);
- switch-door sensors (magnetic);
- cameras;
- Radio Frequency Identification (RFID) tags.

PIR sensors, in particular, represent the most used alternative to obtain information about the state of the environment. They are often used to perceive the movements of people within a certain area. For instance, PIR based sensors are often used (especially with lighting system) for occupancy detection. A first example of how PIR sensors have been used is the *AIM Project* [4], where authors used sensors to get some physical parameters, like temperature and light, as well as PIR to infer user's presence in each room of a house. The authors of [5] uses a deployment of PIR and door sensors to obtain a binary indication of occupancy. They exploit this information to adapt the temperature through a reactive strategy. Moreover they estimate the potential

savings using EnergyPlus. The problem related to PIRs is that they do not give any information regarding how many people occupy the room.

Hence, others technologies can be applied to indoor activity recognition. For instance, in [6], *Erickson et. all* use a 16 node sensor network of cameras (SCOPES) in order to capture occupancy changes among areas with approximately 80% accuracy in real time.

In [7] the authors use a sonar system in order to sense the environment. Relying on the characteristics of the echoes, they deduce a rough map of the focused area. Their system emits a continuous high frequency (ultrasonic) sine wave and records the resulting echoes by using a microphone.

In [8], *Lam et al* conduct their experiments on an extensive testbed that includes distributed sensors for a variety of environment parameters. In particular, the test bed is equipped with CO_2, carbon-monoxide (CO), total volatile organic compounds (TVOC), small particulates (PM2.5), acoustics, illumination, motion, temperature, and humidity sensors.

An even more complete testbed has been constructed in *ARIMA* [9]. Here, to gather data related to total building occupancy, wireless sensors are installed in a three-storey building in eastern Ontario (Canada) comprising laboratories and 81 individual work spaces. Contact closure sensors are placed on various doors, PIR motion sensors are placed in the main corridor on each floor, and a carbon-dioxide sensor is positioned in a circulation area. In addition, the authors collect data on the number of people who log into the network each day. This gives the managers of the building the possibility of being aware of the air quality and of having CO_2 levels indications.

In [10], *Calis et al.* study two ILS (indoor location sensing) built on radio frequency identification (RFID) and on wireless sensor network. They developed two possible algorithms to retrieve pieces of information about the indoor activity of six occupants simultaneously tracked.

We notice that occupancy levels can be inferred also without using PIR or dedicated sensors, by applying system identification and deconvolution techniques on temperature, $CO_2$and actuation levels [11]. These techniques tend to have the convenient property of not requiring dedicated hardware (and thus additional costs).

Summarizing, it is of fundamental importance to provide buildings with monitoring systems dedicated to data acquisition. In fact, a greater knowledge of the controlled environment can be exploited by more advanced control

techniques, that eventually may ensure better comfort conditions without additional energy consumptions.

Methodologies applied on HVAC systems

After discussing the current technologies used in HVAC systems, we overview the methodologies that, exploiting collected data, allow to improve performance of controlling and monitoring systems of buildings. As previously mentioned, occupancy and weather forecasts can be two main conditioning factors to be considered in HVAC control strategies. In the following section we thus summarize the approaches that are used to retrieve pieces of information about occupancy and environment prevision.

Management of information on occupancy patterns As in [12], a first approach is simply to base the control strategies on historical data. Providing the to-be-controlled space with several sensors (motion, temperature, etc.) the authors collected data, and exploited them afterwards to perform occupancy prediction. Depending on the current occupancy state and on previous realization of occupancy pattern, the system decides whether it is convenient to activate a preheating cycle or not. Despite its simplicity, this approach is shown to be more convenient compared to normal thermostat programs.

Another intuitive and simple approach to manage occupancy is to schedule some techniques based both on occupancy and outside temperature knowledge. Several possibilities have been investigated, leading to results that can be satisfactory in many circumstances. Some of the most used scheduling techniques are Interruption, Early Switch Off (ESO), Demand Reduction (DR) and Alternative Switch-On/Off (ASOO). More details on these kind of control strategies can be found in [13].

In [8], an analysis of the correlation between measured environmental parameters and the occupancy level is firstly conducted in order to identify the most significant equipment to get occupancy detection. Moreover *Lam et al.* study the comparison between several approaches for the estimation of indoor activity. In particular they investigate an approach based on Support Vector Machine (SVM), Neural Networks (NN), and Hidden Markov Models (HMM).

In the *AIM* project [4], *Barbato et al.* build user profiles by using a learning algorithm that extracts characteristics from the user habits in the form of

probability distributions. A sensor network continuously collects information about users presence/absence in each room of the house in a given monitoring period. At the end of this monitoring time the cross-correlation between each couple of 24 hour data presence patterns is computed for each room of the house in order to cluster similar daily profiles.

In *OBSERVE* [6], based on data collected by SCOPES system, and the knowledge of room, *Erickson et al.* developed a Markov Chain model in which, the states of the chain consist of the occupancy numbers at each room and transitions can occur according to a time-depending transition matrix.

Management of weather forecasts predictions: Another important information in smart HVAC control is the predicted weather conditions.

In general, predictive strategies (in the sense that account for weather predictions and their uncertainty) turn out to be more efficient and promising compared to conventional, non predictive strategies in thermal control of buildings [14],[15].

In [14] authors have developed both certainty-equivalence controllers using weather predictions and a controller based on stochastic dynamic programming for a solar domestic hot water system. These strategies are based on probability distributions that are derived from available weather data. The simulation results show that these predictive control strategies can achieve lower energy consumptions compared to non-predictive strategies.

In [16] the authors study several methodologies to obtain the correlation between environment scenario and energy needed for HVAC buildings. The approach is based on a detailed analysis of weather sequences and it leads to a classification of climatic situations that can be applied on the site.

Another common strategy is to consider all the uncertain variables acting on the system as the realization of a random process. This approach can be found, for instance, in [17, 18, 15, 19].

In [17] authors exploit predicted future disturbances while maintaining comfort bounds for the room temperature. Both conventional, non-predictive strategies and predictive control strategies are then assessed using a performance bound as a benchmark.

In [18], instead, *Bemporad et. al.* propose a stochastic predictive building temperature regulator where weather and load disturbances are modelled as Gaussian processes. [15] also uses a stochastic MPC and weather predictions.

Firstly it solves a non-convex optimization problem and then it applies a disturbances feedback. [19] finally considers a stochastic approach on the uncertainty of the forecast disturbances (the outside temperature, the occupancy and the solar radiation) solving the problem considering a scenario-based approach and a statistical learning procedure to learn these statistics from real and local data.

1.2 Statement of contributions

This thesis is part of an on-going research project that is developing, implementing and testing MPC techniques on a real test bed. The specific goal of this thesis is to investigate two MPC formulations: the implicit formulation and the explicit one.

This comparison "Implicit MPC- vs. Explicit-MPC" is motivated by economic and application reasons: indeed the Explicit approach tend to be, at least intuitively, more attractive for a possible implementation on real buildings. The main contributions of this thesis are to:

- obtain simpler models of the building dynamics;
- implement the implicit MPC ;
- develop and implement an explicit formulation for HVAC control that uses the simplified model for the thermal dynamic and that takes uncertainty into account;
- investigate the performance of the implicit and explicit MPC through numerical experiments and discuss the results.
- investigate the performance of the explicit MPC with respect to the current practice through experiments on a real test bed

1.3 Thesis Outline

The manuscript is organized as follows. In Chapter 2 we introduce the standard methodologies and tools for the MPC controller. In particular, we describe both the two versions, the explicit MPC and the implicit one. In Chapter 3 we

model the real test bed with two different linear models that couple the two quantities of main interest: the quality of air (in terms of CO_2 concentrations), and the room temperature. Moreover, we obtain a simplified model for the thermal dynamic and we simulate it. In Chapter 4, we introduce our case study and we describe in details the test bed. In Chapter 5 we present actual implemented controllers, the procedures and the necessary control architecture related to the KTH HVAC system. We then present and analyze some results obtained both in simulations and in real experiments in Chapter 6. Finally in Chapters 7 and 8, we draw some conclusions and give some possible suggestions for future investigations.

2

Background on MPC

Model Predictive Control (MPC) has become a standard control method in a wide range of areas. The popularity linked to this approach is due to its flexibility and powerful ability to take into account several constraints and external dynamics that would be hard to include with other approaches.
The basis for this approach can be summarized in a dynamic model as, for instance:

$$x(k+1) = g(x(k), u(k)),\ x(0) = x_0 \tag{2.1}$$

and a cost function to be minimized:

$$\min_{U_N} \sum_{k=0}^{N-1} q(x(k), u(k)) + p(x_N) \tag{2.2}$$

Through dynamic programming algorithm, this problem can be solved giving a solution $U_N = [u(0)^T, \ldots, u_{N-1}]$. The problem is that, in general, the model can be non linear and it describes the dynamic of the plant to control starting from an initial measured state x_0. This is often obtained exploiting identification methods and it is inherently affected by errors with respect to the real process. This is mainly due to either, external disturbances and inaccuracies in the model

construction. To enforce the control strategy the state system is measured after a certain amount of time (e.g a time step), and the dynamic problem solved once again. This procedure endows the system of the required robustness [21].

Hence, this is exactly the main idea behind MPC control that is often called Open Loop Optimal Feedback controller or Reactive Scheduling.

Preliminaries on mathematical optimization problems

In this section,a general introduction to optimization problem is given. The intent, is to give the reader just the necessary background to understand the following part of the thesis.

A general optimization problem is formulated as:

$$\begin{aligned} z^* = \quad & \arg\inf_z \quad f(z) \\ & \text{subj. to} \quad z \in S \subset Z \end{aligned} \tag{2.3}$$

where z collects the decision variables, Z represents the domain of the optimization problem, $S \subseteq Z$ is the set of feasible or admissible decision variables, and z^* is the value of z that solves (2.3). We remark that the optimizer x^* might not be unique.

If we define:

$$f^* := \inf_{z \in S} f(z), \tag{2.4}$$

that is the optimal value of the cost function. In particular the problem (2.3), is said to be *unbounded below* if $f^* = -\infty$, *infeasible* is $S = \varnothing$, and *unconstrained* if $S = Z$.

Among all the possible optimization problems, we are interested just on a specific subclass.

Continuous optimization problems: in these kind of problems, the domain Z, is a subset of the Euclidian vector-space $\mathbb{R}^s$ and the feasible set S, can be defined through a series of inequality and equality constraints.

$$\begin{aligned} \inf_z \quad & f(z) \\ \text{subject to} \quad & g_i(z) \leq 0 \quad \text{for } i = 1, \ldots, m \\ & h_i(z) = 0 \quad \text{for } i = 1, \ldots, p \\ & z \in Z \end{aligned} \tag{2.5}$$

where f, $g_1, \ldots, g_m$, $h_1, \ldots, h_p$ are functions defined over $\mathbb{R}^s$. In this case Z, the domain of the optimization problem, is simply given by the intersection between the domain of the cost function, $f(z)$, and the domain of the inequalities and equalities. Moreover, the feasible set, S is made by all the $z \in Z$ such that all the constraints in 2.5 are satisfied. In particular, we say that $\bar{z} \in Z$, is a feasible vector if $g_{i(\bar{z})\leq 0}$ and $h_j \bar{z} = 0 \; \forall j, i$. Finally, z^*, the optimizer vector, is a feasible vector, with $f(z^*) = f^*$.

Here are two important definitions concerning the constraints.

Definition 1 (Active Constraints)**.** Consider a feasible vector $\bar{z} \in S$, the i-th equality is said to be *active* if:

$$g_i(\bar{z}) = 0 \tag{2.6}$$

Definition 2 (Inactive Constraints)**.** Consider a feasible vector $\bar{z} \in S$, the i-th equality is said to be *inactive* if:

$$g_i(\bar{z}) < 0 \tag{2.7}$$

Other important definitions are those of a convex set, convex function and, finally, convex optimization problem.

Definition 3 (Convex set)**.** A set $S \in \mathbb{R}^s$ is convex if

$$\lambda z_1 + (1-\lambda) z_2 \in S \qquad \text{for all } z_1, z_2 \in S, \lambda \in [0,1] \tag{2.8}$$

Definition 4 (Convex function)**.** A function $f : S \to \mathbb{R}$ is convex if S is convex and

$$\begin{aligned} f(\lambda z_1 + (1-\lambda) z_2) \quad &\leq \quad \lambda f(z_1) + (1-\lambda) f(z_2) \\ &\qquad \text{for all } z_1, z_2 \in S, \lambda \in [0,1] \end{aligned} \tag{2.9}$$

Definition 5 (Convex Optimization Problem)**.** The standard optimization problem as in 2.5 is said to be *convex* if the cost function f is convex on the domain Z and the feasible set S is convex.

The importance of having a convex problem is due either to computational reasons and precision in the solution. In particular, this is due to the following basic theorem which attests that it is sufficient that, in a convex problem, it is sufficient to compute a local minimum to determine the global minimum. Hence, convexity plays an important role in optimization problems and it is exploited also in *nonconvex* that are approximated by convex sub-problems.

Theorem 6 (Solution of a convex problem)**.** Consider a convex optimization problem and let $\bar{z} \in S$ be a local optimizer. Then $\bar{z}$ is *global* optimizer.

The last concept to be introduced in this section is that of *Dual Problem*. This concept will be of paramount importance when will be described the different control methodologies used in this thesis. In particular, the definition of the *Dual Problem*, with respect to the *Primal problem* 2.5, allows to determine a lower bound for the optimal cost f^*.

Definition 7 (Lagrange Dual Function)**.** Consider the non-linear optimization problem 2.5, we define L(z,u,v), the *Lagrange dual function*, in the following way:

$$L(z,u,v) = f(z) + u_1 g_1(z) + \ldots + u_m g_m(z) + v_1 h_1(z) + \ldots + v_p h_p(z), \quad (2.10)$$

The equation can be re-written in a compact way as follow:

$$L(z,u,v) = f(z) + u^T g(z) + v^T h(z) \quad (2.11)$$

If we define the dual cost $\Theta(u,v)$ as:

$$\Theta(u,v) = \inf_{z \in Z} L(u,v,z) \quad (2.12)$$

Then, it is possible to introduce, the Lagrange Dual problem:

$$d^* = \sup_{(u,v),u \geq 0} \Theta(u,v) \quad (2.13)$$

Moreover this Dual problem shows several interesting properties that we give without the proof.

- $\Theta(u,v)$ is *always* a concave function, that implies that the dual problem is always *convex* (maximum of a concave function over a convex set)

- The solution of the dual problem represents a lower bound of the primal problem

$$\sup_{(u,v),u\geq 0} \Theta(u,v) \leq \inf_{z\in S} f(z)$$

. Hence, the difference $f^* - d^* \geq 0$ is called *optimal dual gap*. It is always positive and if $f^* - d^* = 0$ we say that *strong duality* holds and we have zero dual gap.

where the scalars $u_1, \ldots, u_m, v_1, \ldots, v_p$ are called *dual variables* and are all real variables.

Karush-Khun-Tucker Conditions We now introduce a set of *necessary* conditions for any primal-dual optimal pair if strong duality holds and constraints are differentiable, i.e. any z^*, $(u^*,\ v^*)$ must satisfy these conditions.

Theorem 8 (KKT Conditions)**.** Given a general optimization problem 2.5 and its dual 2.19, the primal and dual optimal pair z^*, $(u^*,\ v^*)$ of an optimization problem with differentiable constraints and cost and zero duality gap, has to satisfy:

$$\begin{aligned} \nabla f(z^*) + \textstyle\sum_{i=1}^m u_i^* \nabla g_i(z^*) + \sum_{j=1}^p v_j^* \nabla h_j(z^*) &= 0 \\ u_i^* g_i(z^*) &= 0 \quad i = 1, \ldots, m \\ u_i^* &\leq 0 \quad i = 1, \ldots, m \\ g_i(z^*) &\geq 0 \quad i = 1, \ldots, m \\ h_j(z^*) &= 0 \quad j = 1, \ldots, p \end{aligned} \tag{2.14}$$

Moreover, if the primal problem is *convex* (i.e. linear programming), the KKT conditions are also *sufficient*, i.e., a primal and dual pair z^*, $(u^*,\ v^*)$ which satisfies 2.14 is a primal dual optimal pair with zero dual gap.

Linear Programming: One of the most important subclasses of convex optimization problems, is that of Linear optimization. The main reason for this, is that it is possible to model and solve efficiently a large amount of different problems. In particular, there exist various commercial and non-commercial software available that allow to obtain a solution for these kind of problem in a reasonable range of time.

Definition 9. The intersection $\mathcal{P} \in \mathbb{R}^n$ of a finite set of closed halfspaces in

$\mathbb{R}^n$ is called *Polyhedron*.

$$\mathcal{P} = \{x \in \mathbb{R}^n \ : \ Ax \leq b\} \tag{2.15}$$

If the polyhedron is bounded it said to be a *Polytope*.

Definition 10. The general form of a linear programming problem is:

$$\begin{array}{ll} \inf_z & c'z \\ \text{subj.to} & Gz \leq w \end{array} \tag{2.16}$$

where $G \in \mathbb{R}^{m \times s}$.

We remark that a linear programming problem is always *convex*.

Dual of Linear Programming problem Consider a linear programming problem as in (2.16), we aim to determine the respective dual problem proceeding as explained in the previous paragraph.

First of all we determine the Lagrange function:

$$L(u, z) = c'z + u'(Gz - w) \tag{2.17}$$

and the associated dual cost:

$$\Theta(u) = \inf_z L(z, u) = \inf_z \ c'z + u'(Gz - w) \tag{2.18}$$

and with simple passages we obtain the dual problem:

$$\begin{array}{ll} \inf_u & w'u \\ \text{subj.to} & G'u = -c \\ & u \geq 0 \end{array} \tag{2.19}$$

This concept will be useful when we will introduce the Explicit version of MPC controller that is strongly linked to duality and multi parametric programming.

Preliminaries on Model Predictive Control (MPC)

MPC [20, 21] is a powerful approach to complex and constrained control. How outlined in the introduction to this section, the main idea behind MPC is quite simple. The standard scheme, often called Implicit MPC, requires that, at

every fixed amount of time, an optimization problem is formulated and solved on-line over a determined future window. The outputs of this problem are optimal inputs and theoretical behaviours of the studied plant with respect to an identified model. Basically, an open loop control is set at each sampling time and applied to the system just until the next step. The whole procedure is, hence, repeated basing on the new measurements ans shifting the considered window. This *Receding horizon approach* is what introduces feedback into the system.

For our proposes, the inputs of the optimal problem at each step, would be the heating, cooling, and ventilation commands over the future window. In particular, for slow dynamic system (buildings), this future horizon may coincide with several hours or even days. Moreover, it is quite common in this approach, to include also predictions about upcoming weather, internal gains, control costs or comfort range.

The following Figure 2.1 summarizes the precious discussion giving a global idea of the effective functioning of the MPC controller. A general optimization

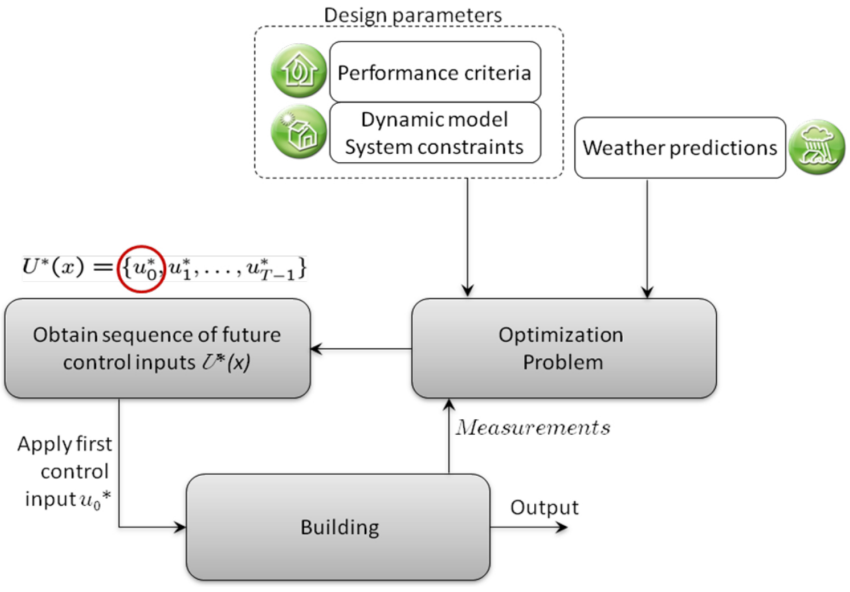

Figure 2.1: Basic description of the main functioning of a Model Predictive Control (MPC) scheme [20].

problem for an MPC approach could be of the form:

$$\begin{array}{lll} \min\limits_{u_0,\dots,u_{N-1}} & p(x_N) + \sum_{i=0}^{N-1} q(x(k), u(k), r(k)) & (1)\ \text{Cost function} \\ \text{subject to} & x_0 = x(0) & (2)\ \text{Current state} \\ & x_{k+1} = f(x(k), u(k)) & (3)\ \text{Dynamics} \\ & (x(k), u(k)) \in \mathbb{X}_k \times \mathbb{U}_k & (4)\ \text{Constraints} \end{array} \tag{2.20}$$

Cost functions

The cost function is of paramount important for two different aspects:

- *Stablity*: it is a common practice to choose the cost function in order to assure stability of the whole system. In the specific case of building, nevertheless, this is not highly required and it is possible to focus just on performances in terms of energy saving.

- *Energy target*: usually the cost function is used to guarantee the maximum in terms of energy performances or in terms of comfort.

Examples are:

$$\begin{array}{ll} \text{Quadratic costs,} & q(x_i, u_i) = x_i' Q x_i + u_i' R u_i \\ \text{Integral costs,} & q(x_i, u_i) = \|u_i\|_1 \\ \text{Probabilistic costs,} & q(x_i, u_i) = \mathbb{E}\big[g\left(x_i, u_i\right)\big]. \end{array} \tag{2.21}$$

The differences between the cost functions lies in what they actually affect. *Quadratic regulators* are mainly used when a trade-off between energy performances and comfort performances is required. *Integral costs* are used when it is more important the energy aspect of the problem. Finally, *Probabilistic costs* can be used to consider the stochastic nature of a real problem.

Dynamics

The Model Predictive Control is a model-based approach. Essentially, based on the current measurement of the state system, a future prediction is obtained through a dynamic model of the real system. This prediction in necessary to compute the optimal solution with respect to a cost function.

It is straightforward to understand that the goodness of the selected model heavily affects the control plans that may eventually lead to poor control

performances. Hence, it is of fundamental importance to choose carefully the predictor model.

Many types of models have been used in this approach, for instance:

$$
\begin{aligned}
&\text{Linear} && x_{k+1} = Ax(k) + Bu(k) \\
&\text{Input-Affine} && x_{k+1} = f(x(k)) + g(x(k))u(k) \\
&\text{Hybrid} && x_{k+1} = \begin{cases} A_1 x(k) + B_1 u(k) & \text{if } x(k) \in P_1 \\ \vdots & \\ A_n x(k) + B_n u(k) & \text{if } x(k) \in P_n \end{cases} \\
&\text{Non-Linear} && x_{k+1} = f(x(k), u(k))
\end{aligned}
\tag{2.22}
$$

Among the aforementioned models, the *linear model* are surely the most widely used. This is due to the fact that they lead to a convex and, hence, easily manageable optimization problem. Both *hybrid models* and *non-linear models* pay in terms of computational complexity the capability to model more complex and general dynamics. Finally, *Input-Affine models*, can cover a large number of very complex systems but are, in general difficult to handle. Nevertheless, it is possible under specific hypothesis, to use mathematical tools in order to make this model easier to handle.

As explained later, the model used in this thesis falls on the last category.

Constraints

The last ingredient of an MPC controller is also the most powerful element of this approach. Indeed, the capability of taking into account several complex constraints is the main reason of MPC success over the years. A generic list of possible implementable constraints is given:

$$
\begin{aligned}
&\text{Linear constraints,} && Ax_i \leq b \\
&\text{Convex quadratic constraints,} && (x_i - \overline{x})^\top P (x_i - \overline{x}) \leq 1 \\
&\text{Chance constraints,} && P(Ax_i \leq b) \leq \alpha \ , \ \mathbb{E}\left[Ax_i\right] \leq b.
\end{aligned}
\tag{2.23}
$$

As well as for the models, also in this case, the most used constraints are the

linear constraints. They allow in particular to specify simple upper and lower bounds on actuation. *Convex quadratic constraints* may arise when bounding total input energy among several actuators. Finally, *Chance constraints*, can be used to bound in a probabilistic sense the behaviour of the inputs as well as the state dynamic. The latter are widely used in this thesis when it comes to stochastic approach to building comfort control.

Another possible approach for MPC: Explicit MPC

The main limitation related with the standard implicit MPC technique is that running the computation algorithm on line at each sample, usually requires substantial computational time. Moreover, keeping in mind the application field of our controllers, the explained procedure might be not attractive for a company. Mainly, this is due to the fact that is often prohibitive to implement an Implicit MPC on a cheap process hardware as a PLC.
One possibility, is to exploit a procedure called Explicit MPC [25, 21]. The main idea of this approach is to solve the optimization problem off-line as a function of the initial state of the system. Hence, we pre-compute the control plan for each x of interest and we store in form of a look-up table or as an algebraic function $u(x) = f(x(k))$. The advantage related with this version of the MPC control is that of reducing the on-line computational effort to a mere function evaluation that can be carried also on cheap hardware. Furthermore, since this new approach provides an insight into the effective control action, it can be advantageous in such circumstances in which high reliability of the controller is required.
To this aim we exploit a mathematical tool called *multiparametric programming*(MP).

Basic Concepts on MP

Firstly we consider a general multiparametric programs of the form:

$$\begin{array}{lcc} J^*(x) & = & \inf_z \ c^T z \\ \text{subj. to} & & g(z,x) \leq 0 \end{array} \tag{2.24}$$

where z is the optimization vector and x is a vector of parameters. The aim is to minimize the cost function that is a function of the parameter x.

We denote as $R(x)$ the set of feasible variables $z \in \mathcal{Z}$ that is:

$$R(x) = \{z \in \mathcal{Z} : g(z, x) \leq 0\} \tag{2.25}$$

while $\mathcal{K}^*$ is the set of feasible parameters:

$$\mathcal{K}^* = \{x \in \mathcal{X} : R(x) \neq \emptyset\} \tag{2.26}$$

Linear mp-Programming Since in our formulation all the constraints are linear we can just focus on a specific class of MP-problems:

$$\begin{array}{lll} J^*(x) & = & \inf_z \ J(z, x) \\ \text{subj. to} & & Gz \leq w + Sx \end{array} \tag{2.27}$$

Given $\mathcal{K} \subset \mathbb{R}^n$ a bounded polyhedral of parameters, following the previous statement (2.26) we can re-write:

$$\mathcal{K}^* = \{x \in \mathcal{X} : \exists z \ Gz \leq w + Sx\} \tag{2.28}$$

Now the aim is to determine the feasible region $\mathcal{K}^* \subseteq \mathcal{K}$, the expression of the value function $J^*(x)$ and the expression of the optimizer $z^*(x) \in Z^*(x)$.
We will use a geometric approach that iteratively divides the parameter space in the so-called *Critical Regions* using KKT conditions [18]

Critical Regions, Dual Problem, KKT conditions Consider the Linear multiparametric program (2.27). Let I be the set of constraints indices (i.e. $I = \{1, 2, \ldots m\}$) we define the critical region CR_A as the set of parameters x for which the subset $A \subset I$ is active at optimum, that is:

$$CR_A := \{x \in \mathcal{K}^* : A(x) = A\} \tag{2.29}$$

where we have defined:

$$\begin{array}{lll} A(x) & := & \{j \in I : G_j z^*(x) - S_j x = w_j \ \forall z^*(x) \in Z^*(x)\} \\ NA(x) & := & \{j \in I : \exists z^*(x) \in Z^*(x) : \ G_j z^*(x) - S_j x < w_j\} \end{array} \tag{2.30}$$

Considering the problem (2.27) and the basic procedure explained in (2.18), we can define the associated dual problem [21]

$$\begin{array}{ll} \min_u & (w+Sx)^T u \\ \text{subj. to} & Gu^T = -c \\ & Gz \leq w + Sx \end{array} \tag{2.31}$$

Firstly we write the primal and dual feasibility conditions and the slackness conditions for the primal and dual problem:

$$\begin{array}{lll} (P.F.) & Gz \leq w + Sx & \\ (D.F.) & G^T u = -c, & u \geq 0 \\ (S.C.) & (G_j z - w_j - S_j x)u_j = 0 & \forall j \in I \end{array} \tag{2.32}$$

Then we choose arbitrarily a specific parameter $x^* \in \mathcal{X}^*$ and we determine the optimal partition $(A, NA) := (A(x^*), NA(x^*))$.
Hence we can rewrite the primal feasibility as follow:

$$\begin{array}{l} G_A z^* - S_A x = w_A \\ G_{NA} z^* - S_{NA} x < w_{NA} \end{array} \tag{2.33}$$

Consider the simplest case of a full-column-rank matrix G_A, we obtain the explicit expression of the optimizer $z^*(x^*)$, that is:

$$z^*(x^*) = G_A^{-1}(S_A x^* + w_A) \tag{2.34}$$

We can also obtain a direct expression of the critical region substituting the previous expression:

$$G_{NA} G_A^{-1}(S_A x^* + w_A) - S_{NA} x^* < w_{NA} \tag{2.35}$$

Moreover we can evaluate the value function in $CR_{A(x^*)}$. In fact since u^*, that is the optimizer of the dual problem, corresponding to x^*, remains optimal, we have:

$$J^*(x^*) = (w + Sx^*)^T u^* \tag{2.36}$$

Now that the critical region has been determined, the next step is to continue exploring the parameter space $R_{rest} := \mathcal{K}^* \setminus CR_{A(x^*)}$. To this aim we introduce the following theorem:

Theorem 11. Let $\mathcal{X} \subseteq \mathbb{R}^n$ be a polyhedron, and $R_0 := \{x \in X : Tx \leq b\}$ a polyhedral subset of X, $R_0 \neq \emptyset$. Also let:

$$R_i = \left\{ x \in X : \begin{array}{l} T^i x > b^i \\ T^j x \leq b^j, \ \forall j < i \end{array} \right\}, \ i = 1, \ldots, m \tag{2.37}$$

where $b \in \mathbb{R}^{m \times 1}$ and let $R^{rest} := \cup_{i=1}^{m} R^i$.
Then:

1. $R^{rest} \cup R_0 = X$
2. $R_0 \cap R_i = \emptyset \ \forall i$
3. $R_i \cap R_j = \emptyset, \ \forall i \neq j$

Hence, basing on the results of the previous theorem, it is possible to explore iteratively the parameter space in the semplified case of absence of degeneracy.

Algorithm 1 Parameter Space Exploration

1: **Execute** *Partition* ($\mathcal{K}^*$)
2: for all regions where $z^*(x)$ is the same and whose union is convex set, compute such a union
3: **end**

Procedure 2 Partition(Y)

1: **if** $\neq x_0 \in Y$: (2.27) is feasible **then**
2: Exit
3: **else**
4: Solve the LP problem with $x^* = x_0$ obtaining z^* and u^*
5: Determine $A(x^*)$ as in Definition (2.30)
6: Obtain $CR_{A(x^*)}$ and $J(x^*)$
7: Partition the rest of the parameter space as stated in Theorem (11)
8: For each non-empty sub-region R_i, execute **Partition**(R_i)

Remark: in this section we obtained an algorithm that iteratively explores the state space obtaining the optimal solution for a given linear program. We notice that the solution can be written as a PWA function of the parameter (i.e. the initial state of the system at each step). Once the computation is done

for all the possible interesting states, we obtain an efficient way to compute the solution of the linear program with respect to a fixed value of the parameter.

The explicit solution obtained in (2.34) can be re written as:

$$\begin{aligned} z^*(x^*) &= G_A^{-1} S_A x^* + G_A^{-1} w_A \\ &= Ex^* + Q \end{aligned} \tag{2.38}$$

where x^* is the considered parameter and the value of E and Q can be easily deduced from (2.38).

Off-Line Complexity and Tractability : we have shown how it is possible to obtain an explicit solution for a programming problem as a function of a parameter.
The main advantage of this approach is to simplify the online computation for a MPC implementation. Nevertheless, this procedure suffers the so-called *curse of dimensionality* [25]. The number of region, computed by the algorithm, increases exponentially with the number of the constraints and is highly sensitive to the dimension of the parameter space. In particular, by considering high dimensional-models may lead to obtain a number of thousands critical region which is not practical in real contest, especially if we aim to achieve a fast and cheap implementation on embedded hardware.

3

Building model and System identification

3.1 Physical modelling

The Model Predictive Control approach inherently requires an appropriate model of the plant to control . Furthermore, this model the model must ensure the right trade-off between precision and simplicity. Precision is required to obtain accurate predictions of the relevant variables, while simplicity, is required in order to ensure computational tractability. Indeed, using a complex model might yield to prohibitive computational procedures or to numerical instability.

Nowadays it is pretty common in the scientific HVAC community to use Building Energy Performance Simulation tools. These tools are extremely sophisticated and precise but they contain complex calculation , non linearities and they can not be used in a building control on line contest. Usually the aim is to find a linear time model that has the major advantage to yield to a convex optimization problem that can be easily solved by one of the current solvers. Hence, it is necessary to our aim to find a simple linear model which describes the plant in the best way.

To cope this problem there are three possible choices

- *Black box identification.* This first technique has the advantage not to assume any knowledge about the plant itself. It relies only on a appropriate input, output data set. Then the parameters of the model are identified in a statistical way thanks to the most common identification methods. If, on one side, this method is conceptually simple, it depends crucially on the availability of an appropriate set of data that is not easy to obtain with real building.

- *Grey box modelling.* This approach use an equivalent Resistance Capacitance model to describe the plant. The topology of the network is determined a priori thanks to the knowledge of the plant. Then the parameters are obtained through identification techniques or using BEPS tools. Compared to the previous method, the latter is to reduce the importance of the data set without assuming a perfect knowledge of the building.

- *White box modelling.* The last method also relies on RC network but this time all the parameters of the network are derived directly from geometry and construction data. It requires availability and processing of building specific information.

Hence, in this chapter, we shall deal with the derivation of a proper model which describes the dynamics of the all the interesting variables involved in the system. Our aim is to obtain two models in order to describe both $CO_2$and Temperature dynamic .

We shall not focus on humidity, due to the fact that in the testbed there is no device capable of modifying its evolution (i.e. there is no dehumidifier or similar devices).

The approach we use is that of white box modelling following the steps of previous works as in [19].

The models are built under the following assumptions:

- no infiltrations are considered, so that the inlet airflow in the zone equals the outlet airflow;

- the zone is well mixed, i.e. the temperature and the concentration of CO_2 are constant with respect to the space and do not depend on the place they are measured;

- the thermal effects of the vapor production are neglected.

Room temperature models

The temperature of the room is calculated via the energy balance of the zone. In particular, the room is modelled as a lumped node and the obtained model is exploitable either in cooling and heating state. The explicit expression follows:

$$m_{air}c_{pa}\frac{\delta T_{room}}{\delta t} = Q_{vent} + Q_{int} + Q_{\text{heat}} + Q_{\text{cool}} + \sum_{\text{j}} Q_{wall,j} + \sum_{\text{j}} Q_{wind,j} \quad (3.1)$$

The equation (3.1) relates the heat exchanges that take place between the various internal and external sources. The left-hand term represents the heat stored in the in the room. Considering the right-hand term, there are all the other heat sources acting on the system. Q_{vent} is the heat flow due to ventilation, $Q_{cooling}$ is the term representing the cooling flows, while Q_{heat} is the heating one. With regard to Q_{int} it contains all the internal heat contributions (number of people, devices, equipment, lightning). Finally, $Q_{wall,j}$ and $Q_{wind,j}$ model the heat contributions due to, respectively, the walls and the windows.

The various contributions in (3.1) can be made explicit:

$$\begin{aligned}
Q_{\text{vent}} &= \dot{m}_{\text{vent}}c_{\text{pa}}\Delta T_{\text{vent}} = \dot{m}_{\text{vent}}c_{\text{pa}}(T_{\text{ai}} - T_{\text{room}}) \\
Q_{\text{int}} &= CN_{people} \\
Q_{\text{heat}} &= A_{\text{rad}}h_{\text{rad}}\Delta T_{h,rad} = A_{\text{rad}}h_{\text{rad}}(T_{mr} - T_{room}) \\
Q_{\text{cool}} &= \dot{m}_{\text{cool}}c_{\text{pa}}\Delta T_{\text{cool}} = \dot{m}_{\text{cool}}c_{\text{pa}}(T_{\text{sa}} - T_{\text{room}}) \\
Q_{\text{wall},j} &= h_i A^j_{wall}(T^j_{wall,i} - T_{\text{room}}) \\
Q_{\text{win},j} &= \frac{(T_{amb} - T_{room})}{R^{\text{j}}_{\text{win}}} + G^{\text{j}}A^{\text{j}}_{\text{win}}I^{\text{j}}
\end{aligned} \quad (3.2)$$

Combining the equation (3.1) with the expression of the terms, we obtain the complete balance equation:

$$\begin{aligned}\frac{dT_{\text{room}}}{dt} &= \frac{\dot{m}_{\text{vent}}\left(T_{\text{ai}}-T_{\text{room}}\right)}{m_{\text{air,zone}}}+\frac{A_{\text{rad}}h_{\text{rad}}\left(T_{\text{mr}}-T_{\text{room}}\right)}{m_{\text{air,zone}}c_{\text{pa}}}\\ &+\frac{cN_{\text{people}}}{m_{\text{air,zone}}c_{\text{pa}}}+\sum_{\text{j}}\frac{h_{\text{i}}A^{\text{j}}_{\text{wall}}\left(T^{\text{j}}_{\text{wall,i}}-T_{\text{room}}\right)}{m_{\text{air,zone}}c_{\text{pa}}}\\ &+\sum_{\text{j}}\frac{\left(T_{\text{amb}}-T_{\text{room}}\right)}{R^{\text{j}}_{\text{win}}m_{\text{air,zone}}c_{\text{pa}}}+\frac{\sum_{\text{j}}G^{\text{j}}A^{\text{j}}_{\text{win}}I^{\text{j}}}{m_{\text{air,zone}}c_{\text{pa}}}\end{aligned} \tag{3.3}$$

The definition of each parameters in (3.3) and their numerical number is shown in the table Table 3.1.

The last thing to do is to model the walls and to describe their dynamic in order to complete the thermal equation (3.3). To this aim we model each wall as two capacitance and three resistance (2C3R system) .the indoor wall temperature $T^{\text{j}}_{\text{wall},i}$ in the j th surface are calculated by means of an energy balance between the outdoor and indoor surfaces. A representation of such a model is shown in Figure 3.1; solving the circuit we can find in/out relationships for wall temperatures. More precisely, such relationships are

$$\frac{dT^{\text{j}}_{\text{wall,o}}}{dt}=\frac{\left[h_oA^{\text{j}}_{\text{wall}}\left(T^{\text{j}}_{\text{ee}}-T^{\text{j}}_{\text{wall,o}}\right)+\frac{\left(T^{\text{j}}_{\text{wall,i}}-T^{\text{j}}_{\text{wall,o}}\right)}{R^{\text{j}}_{\text{wall}}}\right]}{C^{\text{j}}/2} \tag{3.4}$$

$$\frac{dT^{\text{j}}_{\text{wall,i}}}{dt}=\frac{\left[h_{\text{i}}A^{\text{j}}_{\text{wall}}\left(T_{\text{room}}-T^{\text{j}}_{\text{wall,i}}\right)+\frac{\left(T^{\text{j}}_{\text{wall,o}}-T^{\text{j}}_{\text{wall,i}}\right)}{R^{\text{j}}_{\text{wall}}}\right]}{C^{\text{j}}/2} \tag{3.5}$$

The equivalent external temperature T^{j}_{ee} accounts for the different radiation heat exchange due to the orientation of the external walls. The outdoor temperature is modified by the effects of radiation on the j-th wall.

$$T_{\text{ee,j}}=T_{\text{amb}}+\frac{aI^{\text{j}}}{\alpha_{\text{e}}}. \tag{3.6}$$

The parameters present in (3.3) were obtained from in-depth analysis on the room structure, its manufacturing materials and geometrical considerations. The Matlab model has been validated for the Stockholm climate against results from simulation carried out in IDA with climate data from the Swedish

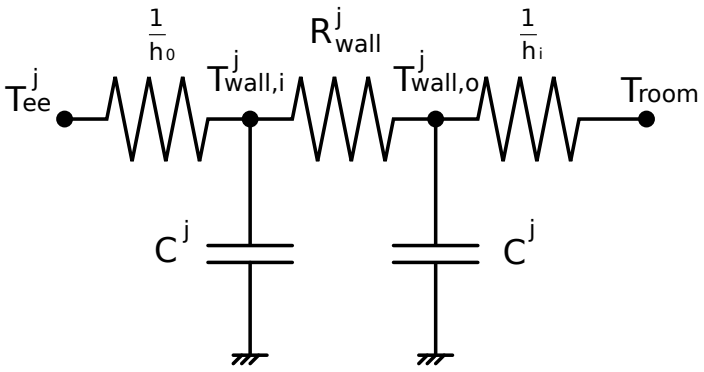

Figure 3.1: Electric scheme of the model of the walls. The three resistances $1/h_{\mathrm{o}}$, $R^{\mathrm{j}}_{\mathrm{wall}}$ and $1/h_{\mathrm{i}}$ are placed between the equivalent temperature $T^{\mathrm{j}}_{\mathrm{ee}}$, and the temperatures $T^{\mathrm{j}}_{\mathrm{wall,o}}$, $T^{\mathrm{j}}_{\mathrm{wall,i}}$ and T_{room}. $R^{\mathrm{j}}_{\mathrm{wall}}$ [°C/W] and C^{j} [J/°C] are the thermal resistance and the thermal capacity of the j-th wall respectively

Meteorological and Hydrological Institute (SMHI). In particular to ensure the validity of the test, the comparison has been performed under the same conditions of ventilation, solar radiation, internal gains and occupancy. Since the aim of this model is to capture the thermal behaviour of the room, heating and cooling processes has been set to zero. In Figure 3.2. the room temperature calculated with Matlab model and IDA is displayed for two months and it shows a satisfactory performance of the obtained model.

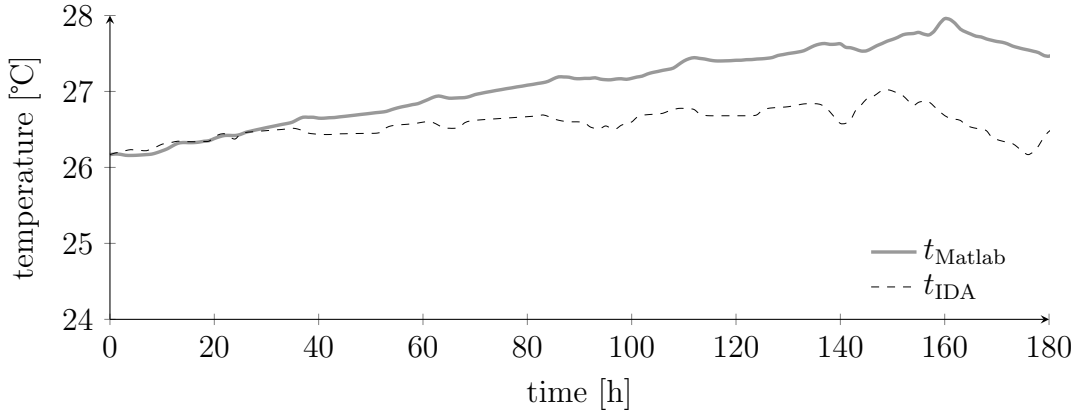

Figure 3.2: Validation of the model performed with the software IDA ICE.

Moreover, a comparison between the model in (3.3) and the actual test-bed was carried out. In this case, it has been considered also the presence of the cooling and heating system. The results, depicted in Figure 3.3 show how the model is not able to fit the the measured data. Nevertheless, for the precision

levels required in this thesis, the model can be considered adequate.

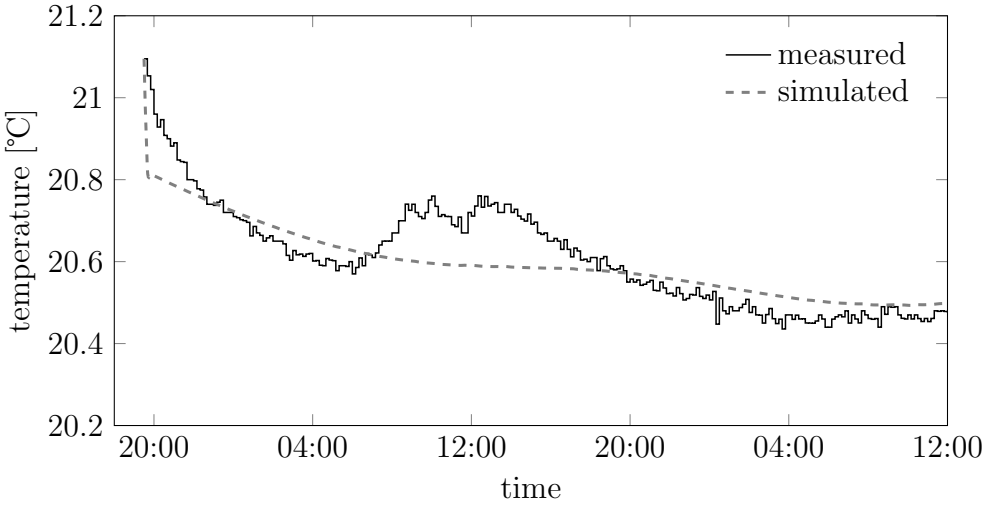

Figure 3.3: Comparison between the simulated temperatures obtained with the physical model and the actual measured room temperature.

Two state model for the thermal dynamic

As shown in the previous section, the model for the thermal dynamics shows trends that can be considered satisfactory. At the same time, however, to describe the complex dynamics such as temperature dynamics, we opted for a system with a quite high dimensions (i.e. 13 states). In a model-based approach control this choice might have repercussions in terms of computation time . How outlined at page 22, especially for the explicit controller, a model of this size could lead to intractability of the problem.
Hence, in this section, we aim to obtain a new model for the thermal dynamic in order to reduce the complexity of the problem. The chosen space state model is based, once again, on a white-box approach.
We model the water tank lab as thermal network made by two nodes. The first one represents the fast dynamic of the air within the room, the second one represents the slow dynamic related to the indoor walls. A schematic of the model used can be found in Figure 3.4.

$$C_a \frac{\delta T_{\text{air}}}{\delta t} = \frac{T_{\text{wall}} - T_{\text{air}}}{R_{\text{aw}}} + \frac{T_{\text{ext}} - T_{\text{air}}}{R_{\text{ae}}} + CN_p + GA_{\text{win}}I \tag{3.7}$$

$$C_w \frac{\delta T_{\text{wall}}}{\delta t} = \frac{T_{\text{air}} - T_{\text{wall}}}{R_{\text{aw}}} + \frac{T_{\text{aver}} - T_{\text{wall}}}{R_{\text{we}}} \tag{3.8}$$

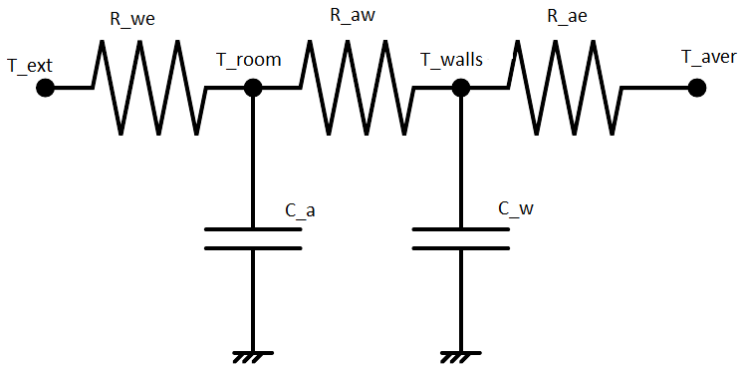

Figure 3.4: Electric scheme for the two state model of thermal dynamic of the room.

where:

- T_{air} is the temperature of the air inside the room;
- T_{wall} represents the average temperature of the walls in the room;
- T_{ext} is the external temperature;
- T_{aver} is the average temperature exciting the system;
- R_{aw} is the thermal resistance between the air and the wall;
- R_{ae} is the thermal resistance between the air and the external temperature (window);
- R_{we} is the thermal resistance between the wall and the external temperature;

To obtain T_{aver} we start for the definition of the disturbances w:

$$w := \left[\begin{array}{cccccc} T_{\text{ext}} & T_{r2} & T_{corr} & T_{r3} & T_{ceil} & I & N_p \end{array} \right]^T$$

hence:

$$T_{aver} := \frac{A_{ext}T_{ext} + A_{r2}T_{r2} + A_{ext}T_{corr} + A_{r3}T_{r3} + A_{ceil}T_{ceil}}{A_{tot}}$$

From the previous formulation (3.7, 3.8) we obtain the continuous linear matrices:

$$\begin{array}{rcl} \dot{x} & = & Ax + Bu + Ew \\ y & = & Cx \end{array} \tag{3.9}$$

where we have defined:

$$x := [T_{air} \quad T_{wall}]^T \quad y := T_{air} \tag{3.10}$$

Hence, the linear matrices are:

$$A := \begin{bmatrix} -\frac{1}{R_{aw}C_a} - \frac{1}{R_{ae}C_f} & \frac{1}{R_{aw}C_a} \\ \\ \frac{1}{R_{aw}C_w} & -\frac{1}{R_{aw}C_w} \end{bmatrix} \quad C := [1 \quad 0]$$

$$E := \begin{bmatrix} \frac{1}{R_{ae}C_a} & \frac{A_{ext}}{A_{tot}}\beta \\ 0 & \frac{A_{r2}}{A_{tot}}\beta \\ 0 & \frac{A_{corr}}{A_{tot}}\beta \\ 0 & \frac{A_{r3}}{A_{tot}}\beta \\ 0 & \frac{A_{ceil}}{A_{tot}}\beta \\ \frac{GA_{win}}{C_a} & 0 \\ \frac{c}{C_a} & 0 \end{bmatrix}^T \qquad B := \begin{bmatrix} \frac{1}{m_{air}} & 0 \\ -\frac{1}{m_{air}} & 0 \\ \frac{1}{m_{air}} & 0 \\ -\frac{1}{m_{air}} & 0 \\ \frac{A_{rad}h_{rad}}{m_{air}} & 0 \end{bmatrix}^T \tag{3.11}$$

where we have defined $\beta = 1/R_{we}$.

To evaluate the obtained model we simulate it against the model presented in 5.8 since, the latter has been validated. In particular, we want to determine and analyse its behaviour under different conditions of actuation, disturbances and occupancy. As it is described subsequently, we are interested in a specific horizon for the predictions. So, the comparison between the two models is calibrated over a period of 24 hours. The results are depicted in Figure 3.5.

The simulations show how the 2-states model is able to capture the dynamic of the more complex 13-states. Obviously, the two graphs are not perfectly overlapped and, there are deviations, between the two, that reach peak value equal to a degree. Despite this, for our purposes, the magnitude of the temperature difference is small enough to take as valid the simplified model.

CO_2 concentration model

For the model of the CO_2 dynamic we follow a grey-box approach. Basically, we describe a physic based model in which all the parameters are identified through the Prediction Error Method Technique (PEM).

Firstly , the CO_2 concentration model has to be specified. In particular,

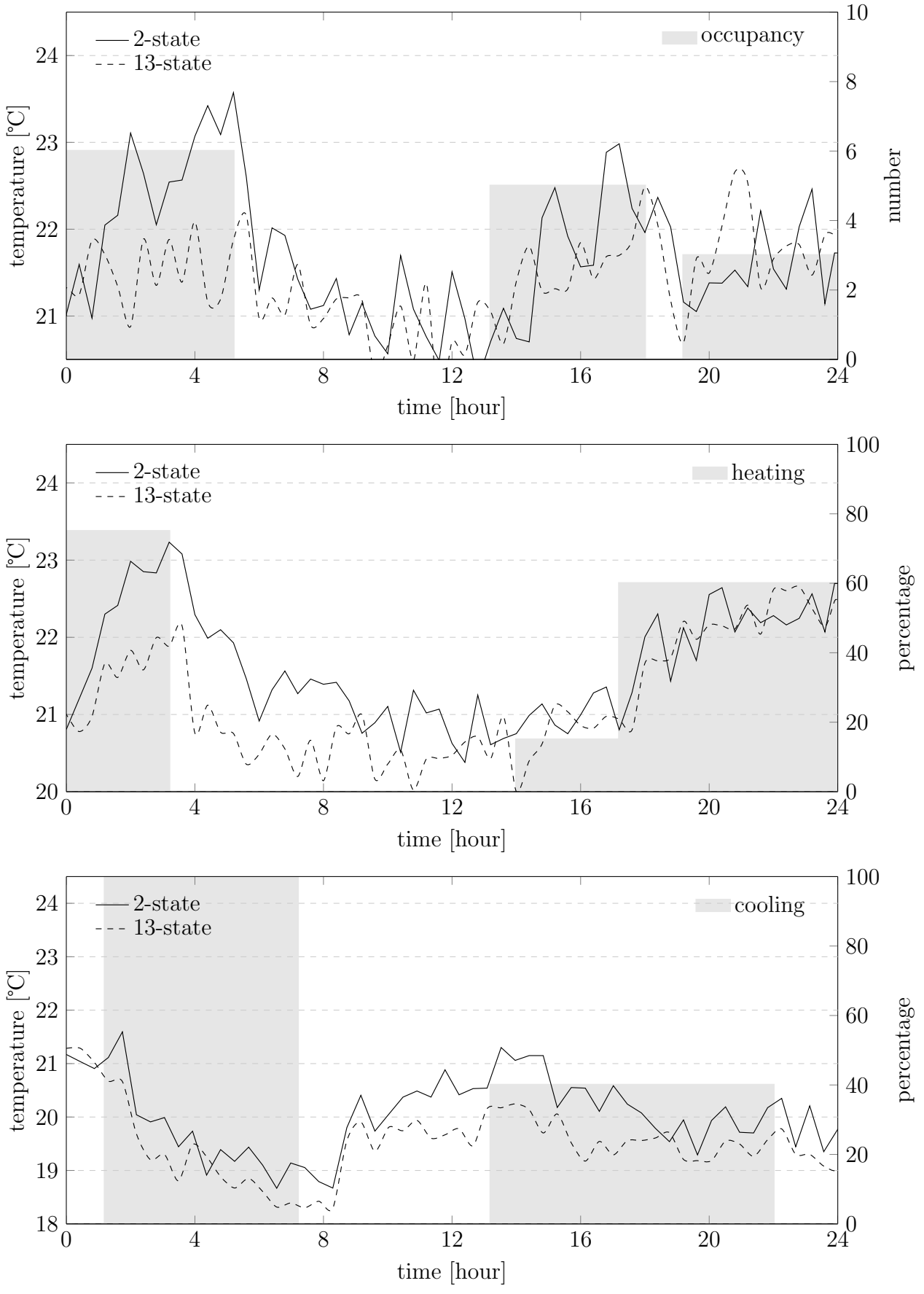

Figure 3.5: Comparison of the two models under different conditions.

the CO_2 level is determined by an equation that balances all the flows that characterize the air inside the room. As previously mentioned, the air within the room is considered to be well-mixed, that means that we assume that the air flowing out has the same CO_2 concentration of the air inside the room. Moreover leakages are neglected, this allows not to consider spontaneous air outflowing.

Hence, from the previous hypothesis, defining $C_{\mathrm{CO_2}}(t)$ as the CO_2 concentration inside the room, C_{in} and C_{out} as the CO_2 concentration of the inflowing and outflowing air respectively and, C_{occ} as the amount of CO_2 due to people in the room, we obtain the following differential equation:

$$V\frac{dC_{\mathrm{CO_2}}}{dt} = C_{\mathrm{in}} - C_{\mathrm{out}} + C_{\mathrm{occ}}. \tag{3.12}$$

where

$$\begin{aligned} C_{\mathrm{in}} &= \dot{m}_{\mathrm{air}} C_{\mathrm{CO_2,i}}, \\ C_{\mathrm{out}} &= \dot{m}_{\mathrm{air}} C_{\mathrm{CO_2}}, \\ C_{\mathrm{occ}} &= g_{\mathrm{CO_2}} N_{\mathrm{people}}, \end{aligned} \tag{3.13}$$

Combining (3.12) and (3.13) we obtain:

$$\frac{dC_{\mathrm{CO_2}}}{dt} = \frac{\dot{m}_{\mathrm{air}} C_{\mathrm{CO_2,i}}}{V} - \frac{\dot{m}_{\mathrm{air}} C_{\mathrm{CO_2}}}{V} + \frac{g_{\mathrm{CO_2}} N_{\mathrm{people}}}{V}. \tag{3.14}$$

Once the balance equation has been introduced, we aim to discretize it through the backward Eulero Method. The difference equation obtained this way is simply:

$$C_{\mathrm{CO_2}}(t_{k+1}) = C_{\mathrm{CO_2}}(t_k) + \frac{\dot{m}_{\mathrm{air}} h_k}{V}(C_{\mathrm{CO_2}}(t) - C_{\mathrm{CO_2,i}}) + \frac{g_{\mathrm{CO_2}} h_k}{V} N_{\mathrm{people}}(t_k). \tag{3.15}$$

where, in particular, $h_k = t_{k+1} - t_k$, has been defined as the considered time step. As said in the introduction to this section, model simplicity is one of the most important aspect to consider when it comes to design an MPC controller . Hence, we chose an ARX model class, whose general form is:

$$A(z^{-1})y(t) = B(z^{-1})u(t) + w(t), \tag{3.16}$$

where $y(t) = C_{CO_2}(t) - C_{CO_2,i} = \Delta CO_2$ represents the difference of the CO_2 between the concentration inside and outside the room, $u(t)$ the input, and $w(t)$ noise accounting fitting inaccuracy and prediction errors. First, we assessed the predictive ability of these models when only occupancy is considered. The considered orders are one regression coefficient on the output, one on the input and one delay. This has be chosen in order to respect the grey-box approach previously introduced. Furthermore, for control reasons, we considered a time step equal to $h_k = 30$ min.

Moreover, we aim to control the Indoor Air Quality (IAQ) regulating the valve opening percentage both of input and output duct. Hence, it has to be taken into account also a term related to the input control. In particular, we define $u(t) = \dot{m}_{air}(C_{\mathrm{CO}_2}(t) - C_{\mathrm{CO}_2,i})$. The resulting model turned out to be:

$$(1 + az^{-1})y(t) = b_1 z^{-1} u(t) + b_2 z^{-1} N_{\mathrm{people}}(t) + w(t) \tag{3.17}$$

In the following Figures are depicted the behaviours of the model obtained through the PEM identification. The results can be considered satisfactory. It has to be noticed, tough, that the assumption of leakages might be a strong hypothesis with respect to the real test bed. Indeed, if we consider the behaviour of the CO_2 concentration within the room, in absence of people and control input, it shows how the air tends to set its CO_2 concentration value to that of the fresh air. Nevertheless, for our purposes, the model is precise enough. Other models have been considered following this approach but they all showed lower performances with respect to the ARX model.

Hence, our adopted model is

$$\Delta_{\mathrm{CO}_2}(t) = +0.8943 \cdot \Delta_{\mathrm{CO}_2}(t-1) - 0.4255 \cdot u(t-1) + 17.9129 \cdot N_{\mathrm{people}}(t-1) + w(t) \tag{3.18}$$

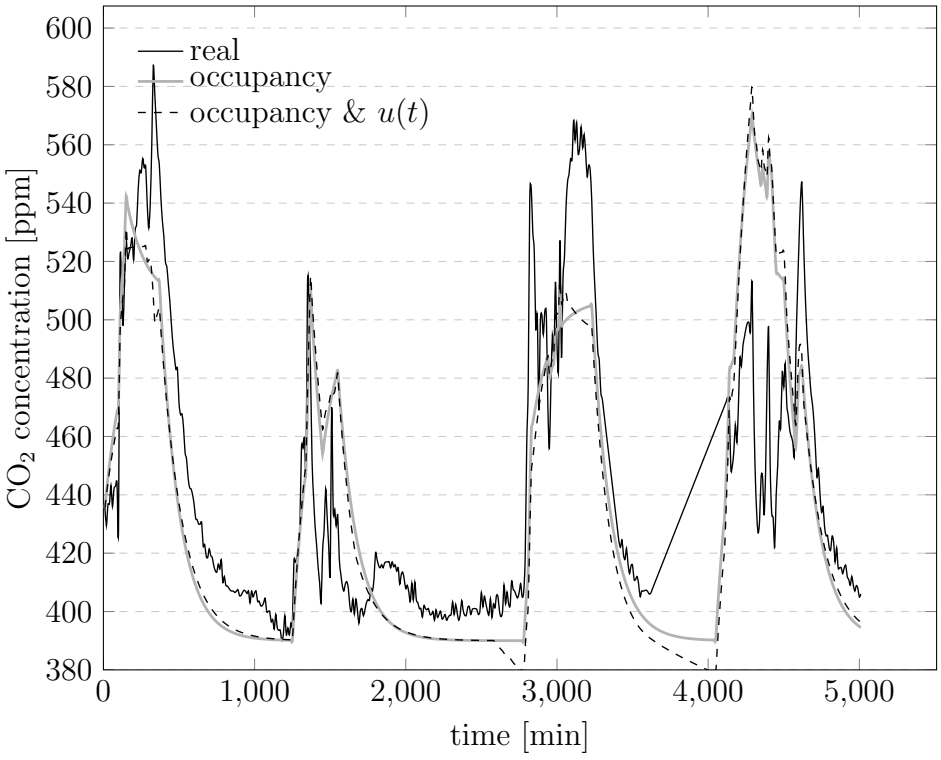

Figure 3.6: Fitting of the CO_2 models with the validation set of data.

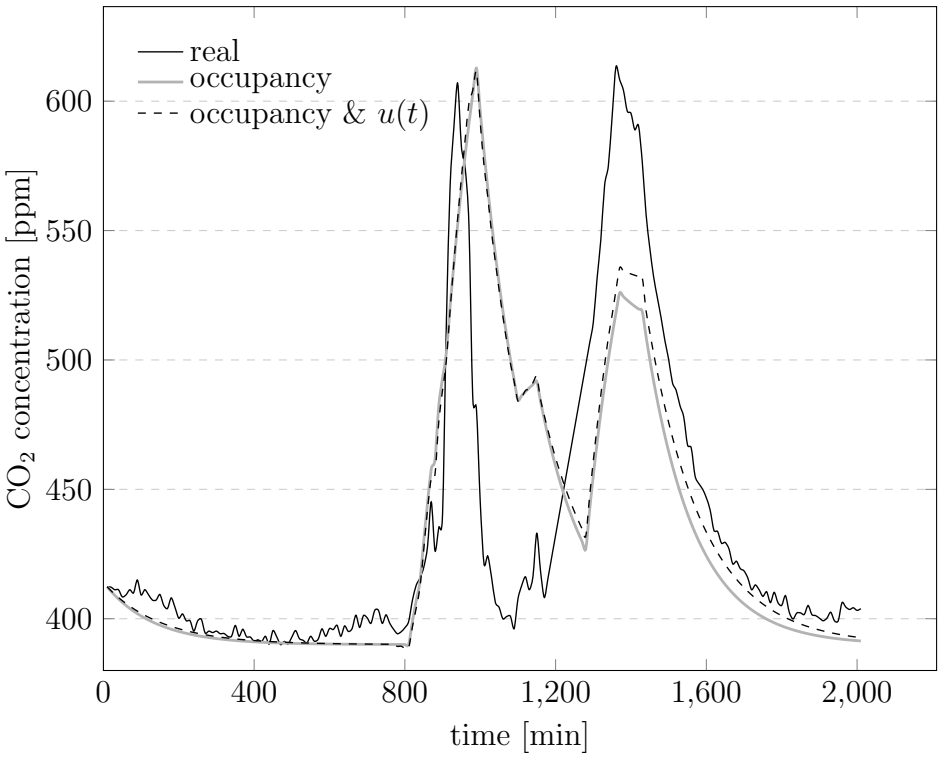

Figure 3.7: Validation of the CO_2 models.

Variable	U.M.	Description
α_{e}	[W/m^2°C]	external heat transfer coefficient
a	[−]	absorption factor for shortwave radiation
A_{rad}	[m^2]	emission area of the radiators
$A^{\mathrm{j}}_{\mathrm{wall}}$	[m^2]	wall area on the j-th surface
$A^{\mathrm{j}}_{\mathrm{win}}$	[m^2]	area of the window on the j-th surface
c	[W]	constant related to equipment and occupants activity
$C_{CO_2,\mathrm{i}}$	[ppmV]	inlet air CO_2 concentration
C_{CO_2}	[ppmV]	concentration of CO_2 within the room
c_{pa}	[J/kg°C]	specific heat of the dry air
g_{CO_2}	[m$^3_{\mathrm{CO_2}}$/pers.]	generation rate of CO_2 per person
G^{j}	[−]	G-value (SHGC) of the window on the j-th surface
h_{i}	[W/m^2°C]	indoor heat transfer coefficient
h_{o}	[W/m^2°C]	outdoor heat transfer coefficient
h_{rad}	[W/m^2°C]	heat transfer coefficient of the radiators
I^{j}	[W/m^2]	solar radiation on the j-th surface
$m_{\mathrm{air,zone}}$	[kg]	air mass in the room
$\dot{m}_{\mathrm{cool}}$	[kg/s]	mass flow through the cooling branch
$\dot{m}_{\mathrm{vent}}$	[kg/s]	mass flow through the ventilation branch
N_{people}	[−]	number of occupants in the room
$R^{\mathrm{j}}_{\mathrm{win}}$	[°C/W]	thermal resistance of the window on the j-th surface
T_{ai}	[°C]	air inlet temperature, from the venting outlet
T_{sa}	[°C]	supply air temperature, from the cooling outlet
T_{amb}	[°C]	outdoor temperature
$T^{\mathrm{j}}_{\mathrm{wall,i}}$	[°C]	indoor surface temperature of the wall on the j-th surface
T_{mr}	[°C]	mean radiant temperature of the radiators
V	[m^3]	volume of the air inside the room

Table 3.1: Summary of the parameters involved in the building model.

4

KTH HVAC TestBed

Description of the system

As underlined in the introduction, it is meaningful to describe and analyze all the characteristics of the actual examined testbed . This is mainly due to the fact that the technologies, environment aspects and peculiarities of the testbed may heavily affect the control strategies and the obtainable results.

The KTH testbed is located in the ground floor of the Q-building of the KTH Royal Institute of Technology campus in Stockholm.

The considered testbed, depicted in 4.2, consists of a main corridor, a conference room, four laboratories, one storage room and the master thesis room. The main goal of the KTH-HVAC project is to monitor the thermal comfort and the Indoor Air Quality (IAQ) of the whole ground floor of the aforementioned building. To this aim, the system is equipped with several sensors on the walls surfaces. In particular, our attention is focused on the temperature and CO_2 levels in each room except the storage room and the PCB lab. Considering Figure 4.2, the server retrieves, through HDH sensors, information on the temperature and CO_2 levels of rooms A:213, A:225, A:235 and A:230. Thanks to this data, the implemented controllers can actuate in

Figure 4.1: External view of the *Q building* in Stockholm, Sweden.

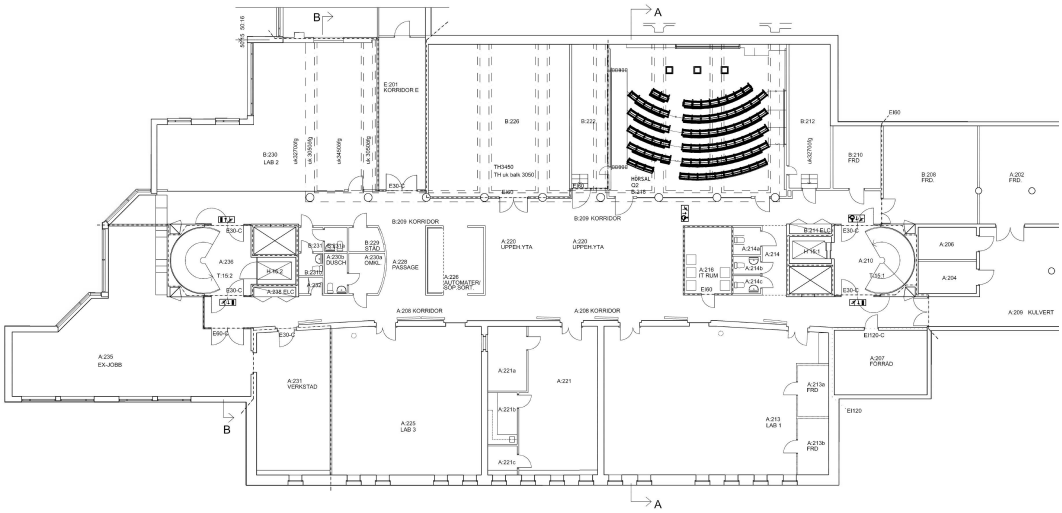

Figure 4.2: Map of the second floor of the Q building. The floor is underground.

order to assure predetermined conditions of thermal condition and air quality.

The Q building is equipped with three separate ventilation units. For the cooling and heating process it relies on a zone-based system. As typical of office areas, the fresh air injected in the building is constant over the period from Monday to Friday and from 7 am to 4 pm.

The processes related to ventilation unit, data acquisition, cooling and heating processes are handled thanks to 3 different Soft PLCs.[1] The product used in the KTH testbed is a Fidelix Soft PLC. This machine can access the Internet and is able to communicate, as an OPC client, to OPC servers, so retrieving all the needed data and communicating also the actuation commands. In particular, the Soft PLCs are programmed to assure a constant temperature of 22^oC with a range of $\pm 1^oC$ and an upper bound for the CO_2 levels (850 ppm). These specifications are given by the KTH environment and building department.

The soft PLCs can be manually controlled using a dedicated Supervisory Control and Data Acquisition (SCADA) system run by Akademiska Hus, a public Swedish company managing academic buildings throughout whole Sweden. This SCADA-based approach is an example of a typical Industrial Control System (ICS) used to monitor and control physical plant. Most of control actions are performed automatically by the PLCs, but the SCADA system allows operators to change set points, enable alarm conditions, and monitor the overall performance of the control loop.

Sub Test Area

As previously mentioned, the KTH HVAC testbed comprises the whole ground floor of the Q building. All the rooms are operationally similar; we thus focus just on the room A:225, informally called *water tank lab*. This room is a laboratory of approximatively 80 m^2 with limited glass surface and one external wall, facing South-East, which is partially shaded by a parking lot.

The room is equipped with an actuation system that is essentially composed of:

- a ventilation system;

[1] Basically, a Soft PLC is a software package which emulates on a normal PC the functionalities of a normal PLC. This brings all the advantages of a normal PC on which is mounted, i.e., flexibility, scalability, and computational power.

- a cooling system;
- a heating system.

Thanks to these systems it is possible to change indoor parameters as temperature, humidity, and CO_2 levels.

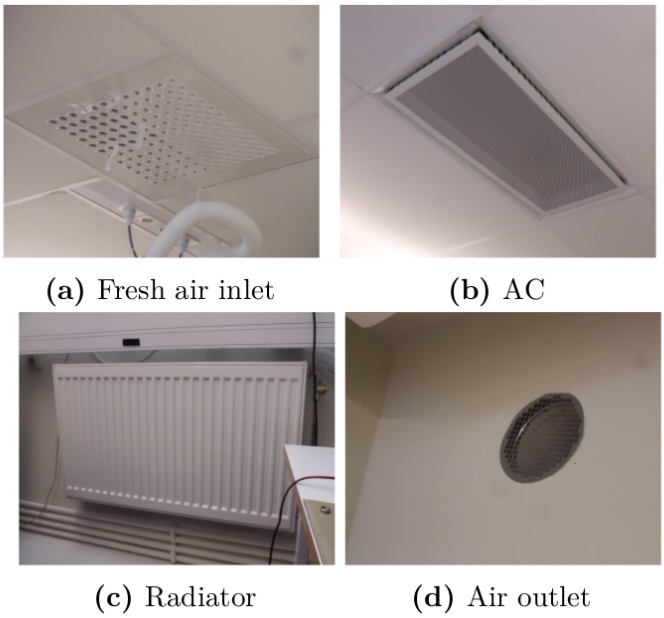

(a) Fresh air inlet **(b)** AC

(c) Radiator **(d)** Air outlet

Figure 4.3: Photos of one of the radiators, the fresh air inlet, the exhausted air outlet and the air conditioning outlet present in the water tank lab.

The following Figure 4.4 shows the schematic of the WTL room in the SCADA system. In addition to Figure 4.5, this schematics allows to understand how the testbed actually works.

- ST901 is the fresh air inlet valve, while ST902 is the exhaust air flow outlet valve. These two valves can control the ventilation system setting the opening percentage.
- SV401 is the valve for the cooling system. Cold water may be imported into the heater exchanger while opening SV401.
- SV201 is the radiator valve. It allows water to circulate through radiators pipes.
- GN501 is the occupancy sensor with a boolean output. Green light represents an "occupied" state while white light represents a "not occupied" state.

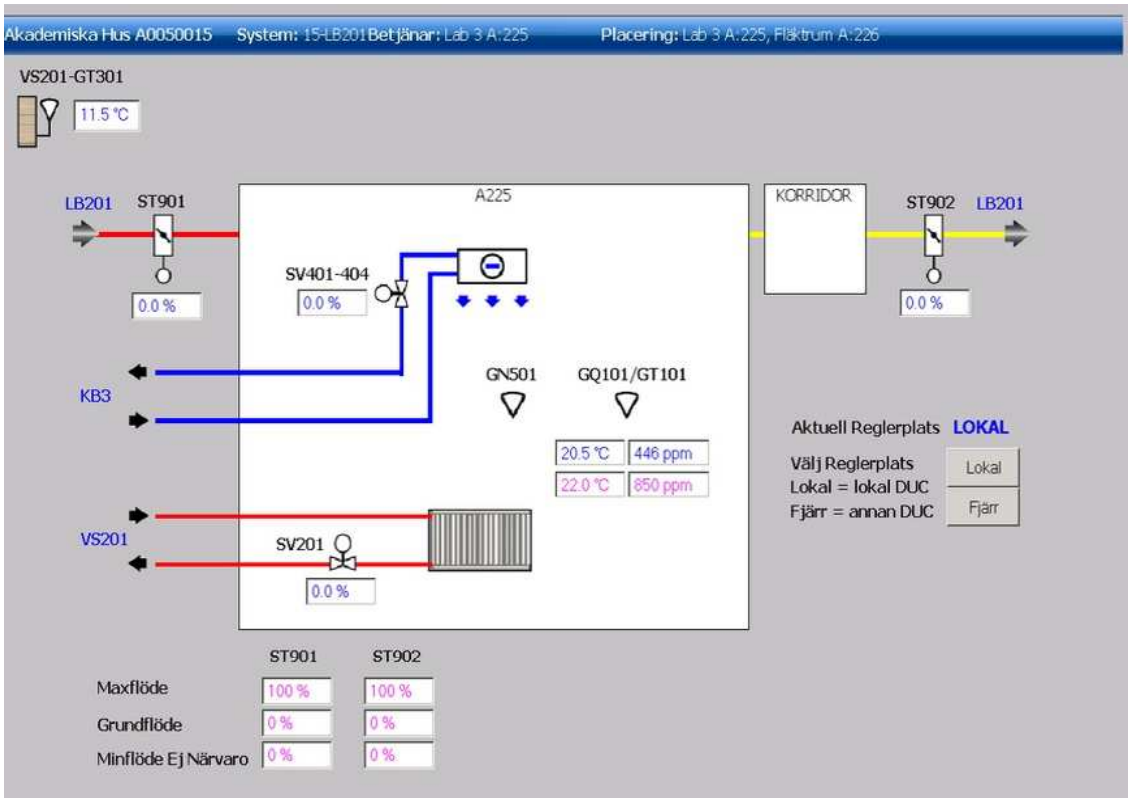

Figure 4.4: Schematic of the Water Tank Lab in the SCADA system.

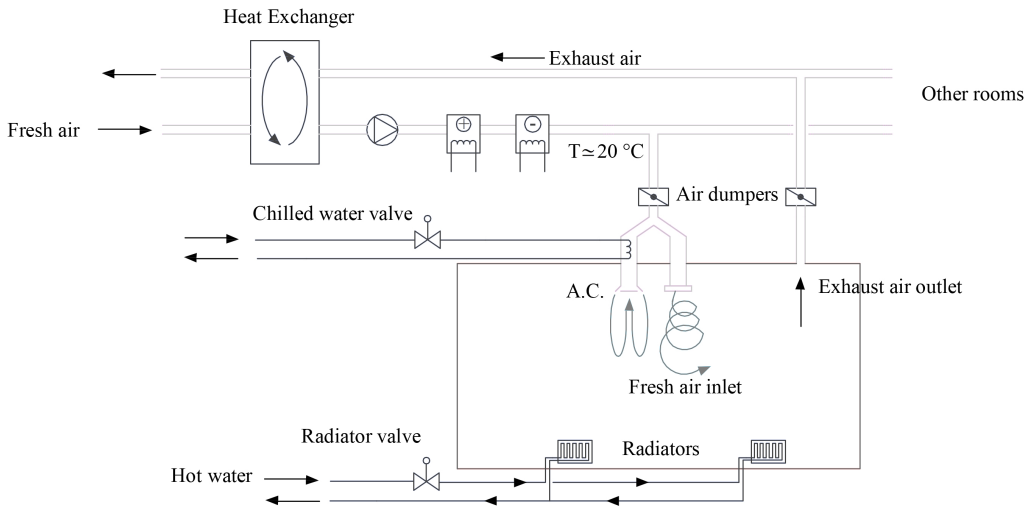

Figure 4.5: Diagram of the actuation systems present in the water tank lab. This scheme shows the degrees of freedom and the constraints that must be faced when designing air quality control schemes for the considered testbed.

- GQ101/GT101 represent CO2 and temperature sensors respectively.

- Lokal/fjarr are Swedish words that mean Local/Remote. Switching to Fjarr mode the operator can actually control the room while in the Lokal mode a default controller (Akademiska Hus's) is set.

The heating subsystem

The heating system is implemented through the use of common radiators. In particular, in the A:225 room, four double-pipe radiators are installed. As it is normal for this kind of heat exchangers, hot water (generated separately) is made circulating through radiators by means of a pump. One aspect to be noticed is that the hot water exploited in this heating process comes from a district heating system, a system for distributing heat generated in a centralized location for residential and commercial heating requirements.

Notice that this is a quite common practice in the Nordic countries, since it allows to divide the generation of heat from its usage, and this overall allows energy efficiency. The sources used to achieve heating generation are usually burning fossil, biomass, nuclear power but also renewable energy sources.

The fact that the *hot water circulating the radiators pipes is provided by an external heating system* is meaningful because it has an important consequence in the control process. The actual temperature of the flowing water is indeed given by the district heating as a static map of the outside temperature. The controller can access only a valve placed before the first radiator and whose opening percentage affects the amount of actual water circulating through the pipes.

This map is shown in Figure 4.6.

The venting and cooling subsystem

As previously mentioned, in the Q building fresh air is supplied by means of three separated ventilation units. The provided fresh air is normally between 20 and 21 degrees and it supplies both to the venting and cooling system. Another time, it is crucial to notice that the *air flowing the Q building is regulated by an external system and the period of activity is limited between 7.00 am and 4 pm*. This is fundamental when considering the actual possibilities of control.

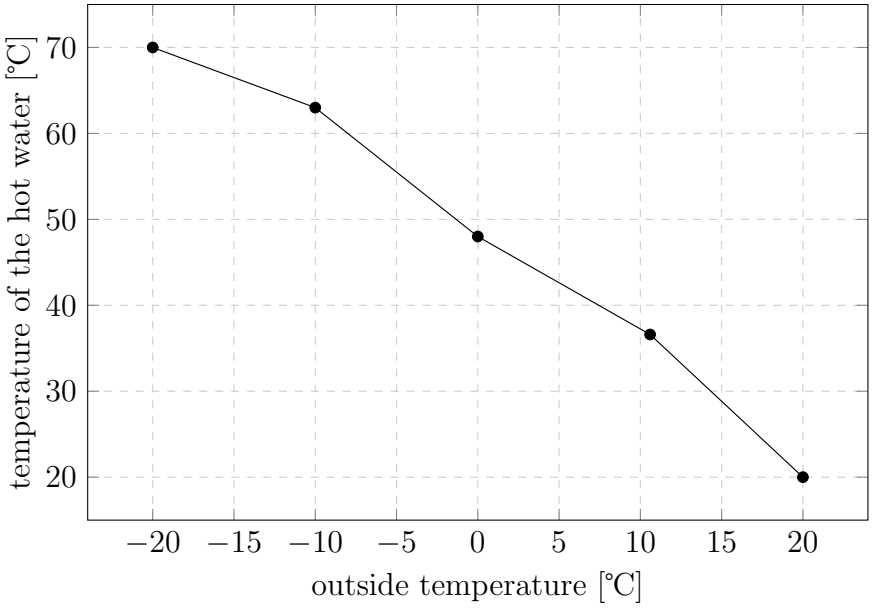

Figure 4.6: Map showing the temperature of the water flowing through the radiators as a function of the external temperature.

The ventilation system The ventilation system can be divided into two fundamental parts: the first regulating the fresh air coming into the room, and the second determining the air going out of the room. The amount of fresh air, coming from one of the ventilation units, is regulated by a dumper as depicted in Figure 4.7 while the exhaust air can simply flows through a hole in the wall in which another dumper can determine the opening percentage.

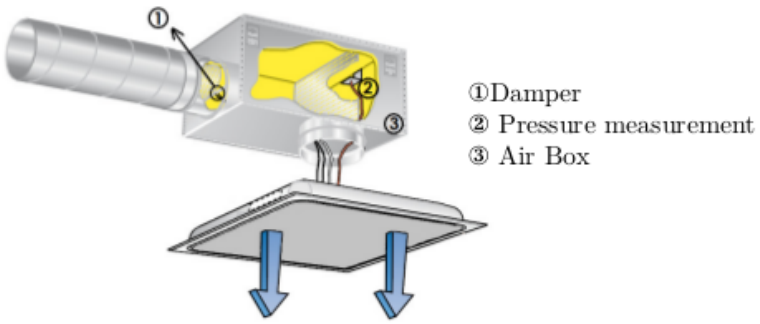

Figure 4.7: Scheme of the air inlets present in the water tank lab.

The cooling system With reference to the Figure 4.8, in this paragraph it is described the functioning of cooling system. Basically, the cooling process is based on the induction principle. The fresh air provided by one of the

ventilation units is injected into a plenum, a housing where it is created and stored air with a greater pressure than the atmospheric one. In this plenum nozzles of various sizes are deployed; these allow the system to discharge the air. Thanks to the high pressure in the plenum, the air comes out through the nozzles at a high speed and it creates a zone with lower pressure. This depression causes the room air to be aspired through the heat exchanger. In particular, in the heat exchanger, chilled water flowing into the coil allows to cool the air previously aspired. The cooled air is eventually mixed with the primary air and discharged into the room from the sides of the devices.

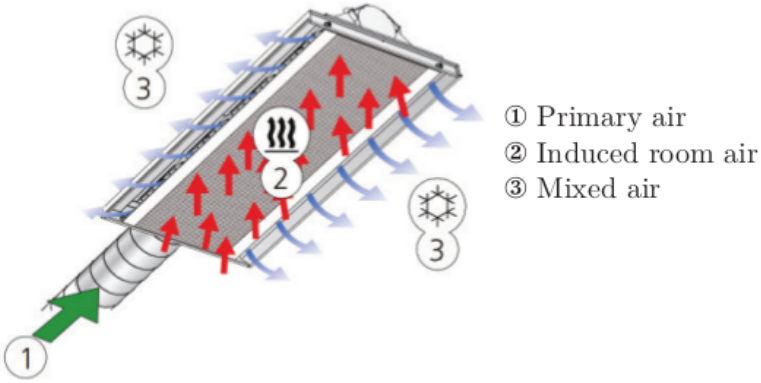

Figure 4.8: Scheme of the air conditioning system of the water tank lab.

Moreover, the AC unit can be used to heat the room. In this case, the water circulating the coil, is warm. This heating process is, however, more costly with respect to the heating given by the radiators. Another aspect to consider is that, as for the radiators system, the water circulating in the coil is not directly modifiable. Its temperature depends statically on the outside temperature. The average temperature of the water measured in the water tank lab corresponds at 16℃.

Continuing the analogy with the heating system, actuation of the cooling subsystem is performed through a valve that is placed before the chilled water circuit and whose opening percentage can be set using the SCADA web interface.

Another aspect to be noticed is the close link between ventilation and cooling system. Even in the case in which the cooling process is not required, fresh air is injected into the room through cooling unit nozzles. In particular, the amount of fresh air circulating corresponds to 30% of the total available air.

The main consequence of this peculiarity is that: the cooling system to be active needs the ventilation system to be active; this means that *when the ventilation system is deactivated it is not possible to perform cooling in the room.*

Effects of the ventilation on the cooling/heating As described before, the ventilation system affects both the heating and cooling processes. Figure 4.9 shows the entire air process in the schematic version that the user finds on the SCADA web interface.

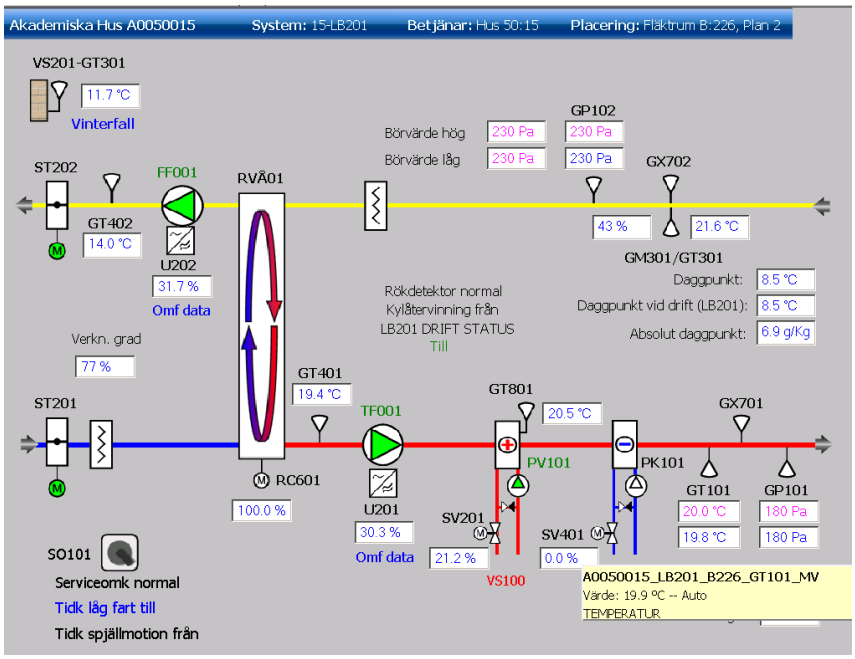

Figure 4.9: SCADA interface of the system that provides the fresh air to the venting and cooling system

The previous processes can be summarized as follows:

1. the fresh air from outside is imported through a valve (denoted with the code ST201);

2. the air is then filtered by appropriate filters;

3. after that the air is processed by a heater exchanger which exploits the heat of exhaust air flow. As shown in the Figure 4.9 the imported fresh air is warmed up to 19.4℃;

4. the pump TF001 then pushes the warmed air to the heating and cooling system sequentially; due to this the temperature of the fresh air that flows through the ducts is around 20℃ in each room;

5. the fresh air is eventually discharged into the rooms at a temperature that is always around 20℃.

Summarizing, when the temperature of the room is below 20℃ the air from the ventilation helps the heating system to increase the indoor temperature. Otherwise, if the temperature is greater then 20℃the ventilation system helps to lower the room temperature.

Sensors and Forecast

WSN

In a control system is of paramount relevance to obtain the current state of the controlled plant. To this aim, besides the data gathered through the HDH sensors, in our testbed is implemented a wireless sensors network using motes. These *Tmote Sky* devices include a number of on-board sensors to measure light, temperature and humidity. In addition of that, other external sensors may be connected to the motes (i.e CO_2 sensor), using the dedicated ADC channel on the opportune expansion area.

An example of T-Mote is reported in Figure 4.10.

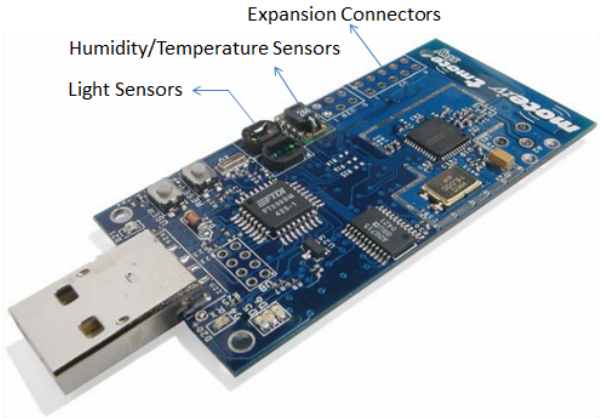

Figure 4.10: A Tmote Sky with highlighted the various measurements systems.

In Figure 4.10 all the sensors currently used are depicted. The red ones are placed inside the room, the blue one is put outside building and the green one is in the corridor. All them follow star network topology to send data to root mote which is marked as black in the Figure 4.11.

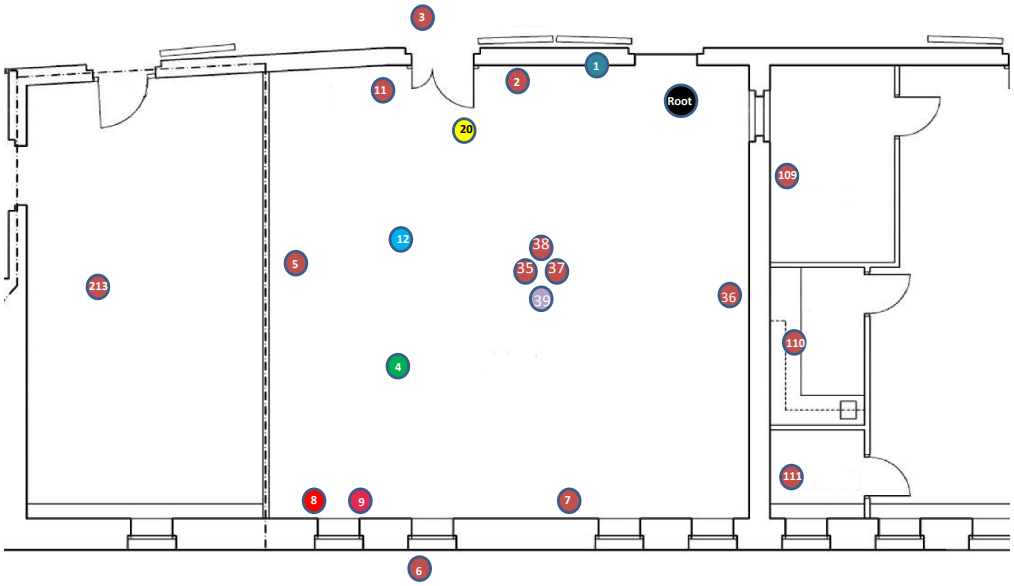

Figure 4.11: Map of the sensors deployed in the KTH testbed

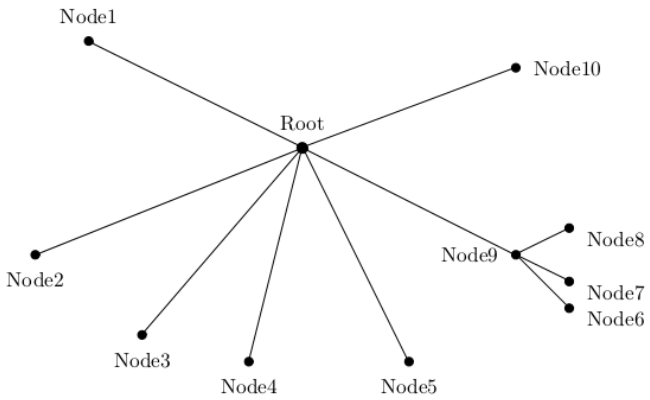

Figure 4.12: Tipical star network topology, it is used also in our network

The motes forwards the sensed data to the main server every 30 seconds. The list of the nodes and of their main features are summarized in Table 4.1.

Mote Id	Spot	T	H	C	L	Description
1002	WTL	√	√	-	-	Environment
1003	Corridor	√	√	-	-	Corridor
1005	WTL	√	√	-	-	Indoor wall temperature
1006	Outside	√	√	-	-	Outdoor wall temperature
1007	WTL	√	√	-	-	Room wall temperature
1008	WTL	√	-	-	-	Attached to the radiator inlet
1009	WTL	√	-	-	-	Attached to the radiator outlet
1011	WTL	√	√	-	-	Room wall temperature
1012	WTL	√	√	-	-	Air conditioning outlet
1020	WTL	-	-	-	√	Environment
1033	WTL	√	√	-	-	Environment, attached to the floor
1036	WTL	√	√	-	-	Room wall temperature
1037	WTL	√	√	-	-	Ceiling
1042	WTL	√	√	√	√	Near exhaust air outlet
1043	WTL	√	√	√	√	Environment
1047	WTL	√	√	√	√	Near fresh air inlet
1110	PCB Lab	√	√	-	-	Attached to wall
1213	Storage room	√	√	-	-	Attached to wall

Table 4.1: Summary of the mote of the WSN (T, H, C, L stand for temperature, humidity, CO_2 and light respectively)

People counter

In order to measure occupancy the testbed is provided with a photoelectric based people counter. This kind of device represents a valid alternative to this aim because of its low cost and high privacy level respect other technologies.

The device consists of three sensors. In particular, there are two photoelectric sensors and a magnetic sensor.

The photoelectric sensor, showed in the Figure 4.13 , is a retro-reflective sensor ML 100-55/102/115 with polarization filter, plastic housing and 5m detection range. The magnetic sensor, Figure 4.14 is the 1108 Hall-Effect sensor that provides a voltage output that is proportional to the magnetic field.

The two photoelectric sensors are mounted on the outside of the entrance door. They output low level when people pass through the door. the magnetic sensor is used to determine whether the door is opening or closing. Eventually all the sensor are connected to the expansion connectors of TmoteSky through cables. This node stores acquired data in a circular buffer and sends it to the Base Station node.

Figure 4.13: Photoelectric device used in the people counter system.

Figure 4.14: Magnetic device used in the people counter system.

Weather forecasts

As highlighted in our literature review, the knowledge of the future outdoor conditions is crucial for achieving good control performance in terms of energy savings. To this aim the testbed server fetches and stores information the web site `www.wunderground.com`. More precisely, the available data are:

- temperature (current and the hourly forecasts for the next 72 hours);
- wind speed (current and the hourly forecasts for the next 72 hours);
- wind direction (current and the hourly forecasts for the next 72 hours);
- wind gusts (only the current status);
- precipitation (current and the hourly forecasts for the next 72 hours);
- external air pressure (only the current status).

Central PC and LabVIEW

The pulsing heart of the testbed is located in a dedicated server running in the water tank lab (WTL). This server implements all the logic that allows the user to perform all the possible communications with the various devices. The instruments that make these communications possible have been designed and developed in LabVIEW. The server is connected through Ethernet cables to the KTH network and to the external Programmable Logic Controller (PLC), and is reachable through dedicated TCP-IP Internet ports. A schematic representation of the whole communication system is shown in Figure 4.15.

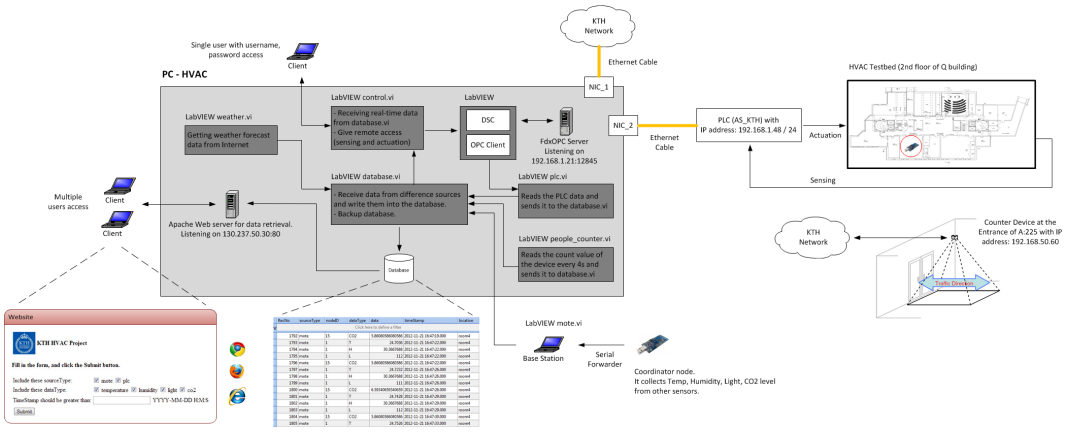

Figure 4.15: A scheme representing the whole testbed system; LabVIEW is the tool that allow the user to communicate with the whole network by a collection of virtual instruments.

5

Control strategies

In this chapter the various types of control applied to the system are introduced and described. Firstly, the default controller is briefly analyzed. This controller, developed by an external entity, is basically a PID controller. Afterwards, a more advanced control scheme, Model Predictive Control, is presented in both the versions implemented in this thesis.

5.1 The current practice Proportional Integrative (PI) controller

The current practice is to apply a simple PI control. In particular the system operator, Akademiska Hus, implemented two different PI controllers, one of them supervising the IAQ, i.e. the CO_2 concentration of the air, the other one supervising the indoor room temperature. A brief description of the actual operation process is given in the following. It has to be noticed that a precise documentation of the implemented controllers is still missing and just general descriptions can be given.

Temperature controller: the temperature controller uses the actuation present

in the lab in this way: during winter season it uses the heating system, while during the summer season it exploits the cooling system. The control actuation can be activated just when the temperature of the room does not lay in a comfort band that represents the desired temperature range. Basically, the controller is programmed not to assure the temperature to follow a temperature reference but rather to assure the temperature to be inside a band of comfort. This is season-changing and it is set to be $[21 - 23]$ ℃during the summer and $[20 - 22]$℃during the winter. The working frequency for the controller is equal to one command per second. We notice that this control strategy does not take into account neither energy efficiency nor actuators wear indexes;

CO_2 levels controller: this controller actuates only the ventilation system. The control strategy is similar to the previous one, with the CO_2 ppm levels dead zone that ranges from 0 to 850.

In Figure 5.1 is depicted the behaviour of the aforementioned controller. We can notice that the controller do not respect the indications given in Academiska Hus' documentation and that the controller suffers from actuation peak problems as well as out of bound temperature values.

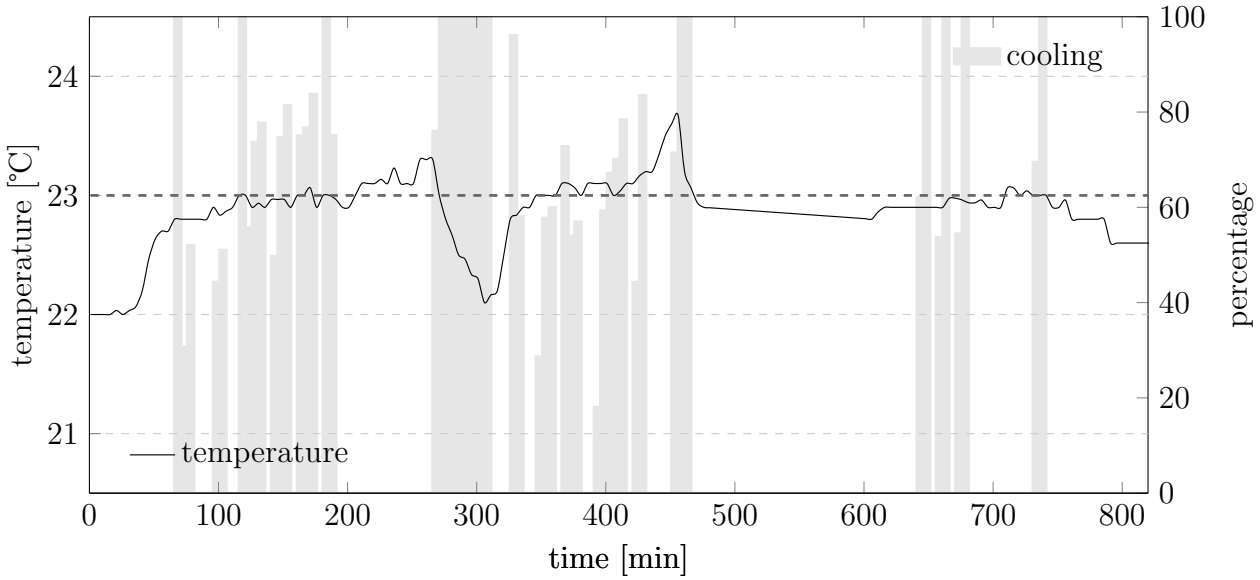

Figure 5.1: Example of the actuation signals induced by the Akademiska Hus PI controller: heating action.

5.2 The MPC implemented in the testbed

With respect to the general introduction given in the chapter 2, we want now to present the specific peculiarities of our MPC controller. Initially, an on-line implementation of the MPC controlled is followed [22]. Subsequently, another possibility is explored, that is an off-line implementation of the controller.

General aspects

- we chose an *integral cost* function in order to focus on energy performances;
- a *linear dynamic* is assumed to achieve computational efficiency;
- just *linear constraints* are considered. In particular, we want to restrict actuation values as well as satisfy comfort requirements on IAQ and room temperature.

To improve tractability of the whole control problem we exploit the independence of the CO_2 concentration from the thermal one. Hence, we split the problem in two different sub-problems that work in cascade: CO_2 -MPC problem which aims to keep the concentration within comfort bounds while minimizing energy consumption; T-MPC problem which focuses on the room temperature.

The models (3.3) and (3.18) described in Section 3.1 contain non-linearities that can lead to intractable problems. To address this issue we derive linear equivalent formulations of the CO_2 concentration model (in Section 3.1) and of the room thermal model (in Section 3.1) [22].

CO_2 Linear Model The aim of this paragraph, is to obtain a linear model for the CO_2 concentration starting from the non linear model (3.15). As already considered in (3.18) , we replace the non-linear term $\dot{m}_{\text{air}} \cdot (C_{\text{CO}_2} - C_{\text{CO}_2,i})$ with u_{CO_2}, where $C_{\text{CO}_2,i}$ is the concentration of the air that is flowing inside. Moreover we assume it as a constant set to an average value of 450 ppm. Since $C_{\text{CO}_2,i}$ is the minimum level that the indoor air may have, $C_{\text{CO}_2} - C_{\text{CO}_2,i}$ is a non-negative variable. Hence, the CO_2 concentration dynamics can be described by the discrete LTI system:

$$\begin{aligned} x_{CO_2}(k+1) &= a x_{CO_2}(k) + b u_{CO_2}(k) + e w_{CO_2}(k) \\ y_{CO_2}(k) &= x_{CO_2}(k), \end{aligned} \tag{5.1}$$

where

$$x_{CO_2}(k) = C_{\mathrm{CO}_2}(k) - C_{\mathrm{CO}_2,i} = \Delta CO_2$$

is the state, and

$$w_{CO_2}(k) = N_{\mathrm{people}}(k)$$

is the disturbance at time step k. The values of the parameters present in (5.1) can be found in (3.18).

Temperature Linear Model Also in this case, we aim to obtain a linear model. Considering the model presented in Section-3.1, we want to hide the bilinear term of the indoor dynamics Q_{vent}, Q_{cool} and also, model the contribution due to requirements CO_2 concentration levels [1].

Starting form the definition of Q_{vent} and Q_{cool}:

$$\begin{array}{rcl} Q_{\mathrm{vent}} & = & \dot{m}_{\mathrm{vent}} c_{\mathrm{pa}} \Delta T_{\mathrm{vent}} = \dot{m}_{\mathrm{vent}} c_{\mathrm{pa}} (T_{\mathrm{ai}} - T_{\mathrm{room}}) \\ Q_{\mathrm{cool}} & = & \dot{m}_{\mathrm{cool}} c_{\mathrm{pa}} \Delta T_{\mathrm{cool}} = \dot{m}_{\mathrm{cool}} c_{\mathrm{pa}} (T_{\mathrm{sa}} - T_{\mathrm{room}}) \end{array} \tag{5.2}$$

we define:

$$\begin{array}{rcl} Q_{\mathrm{air}} & = & Q_{\mathrm{vent}} + Q_{\mathrm{cool}} = \dot{m}_{\mathrm{air}} c_{\mathrm{pa}} \Delta T_{\mathrm{air}} \\ & = & \dot{m}_{\mathrm{air}} c_{\mathrm{pa}} (T_{\mathrm{air}} - T_{\mathrm{room}}) \end{array} \tag{5.3}$$

where, in particular, T_{air} represents the result of the interaction between the temperature of the air from the venting outlet, T_{ai}, and the air coming from the cooling outlet, T_{sa}.

Once modelled the total heat due to the ventilation system, we want to take into account the lower bound of the CO_2 problem.

$$Q_{\mathrm{air}} = \dot{m}_{\mathrm{air}}^{CO_2} c_{\mathrm{pa}} (\Delta T_h - \Delta T_c) + c_{\mathrm{pa}} (\Delta u_h - \Delta u_c) \tag{5.4}$$

In this way, we have decoupled the two problems. This approach leads, nevertheless, to add a greater number of inputs with respect to the original problem. It is crucial to understand the meaning of the non-negative variables ΔT_h ΔT_c

[1] We remark that the problem are solved in cascade. Hence, the output of the C-MPC represents an input for the T-MPC.

Δu_h Δu_c that are subjected to:

$$\begin{aligned} \Delta T_h - \Delta T_c &= T_{\text{air}} - T_{\text{room}} \\ \Delta T_h + \Delta T_c &= |T_{\text{air}} - T_{\text{room}}| \\ \Delta u_h - \Delta u_c &= \Delta \dot{m}_{\text{air}}(T_{\text{air}} - T_{\text{room}}) \\ \Delta u_h + \Delta u_c &= \Delta \dot{m}_{\text{air}}|T_{\text{air}} - T_{\text{room}}| \end{aligned} \tag{5.5}$$

with:

$$\Delta \dot{m}_{\text{air}} = \dot{m_{\text{air}}} - \dot{m}_{\text{air}}^{CO_2} \tag{5.6}$$

that models the additional air flow rate required from the T-MPC problem to satisfy thermal bounds.

The LTI system describing the thermal dynamic of the room can be defined.:

$$\begin{aligned} \dot{x}(t) &= A_c x(t) + B_c u(t) + E_c w(t) \\ y(t) &= C_c x(t), \end{aligned} \tag{5.7}$$

where all the matrices in 5.8 can be found in the Appendix.

$x(k) \in \mathbb{R}^{13}$ is the state vector containing the room temperature and the inner and outer temperatures of all the walls,

$$x(t) = \begin{bmatrix} T_{room} & T^1_{wall,o} & T^1_{wall,i} & \dots & T^6_{wall,o} & T^6_{wall,i} \end{bmatrix}^\top$$

$u(k)$ and $w(k) \in \mathbb{R}^3$ are the vector of our inputs and the vector of random disturbances at time k respectively

$$\begin{aligned} u(t) &= [\Delta T_h(t)\ \Delta T_c(t)\ \Delta u_h(t)\ \Delta u_c(t)\ \Delta T_{h,\text{rad}}(t)] \\ w(k) &= [T_{\text{amb}}(t)\ I^1(t)\ N_{\text{people}}(t)] \end{aligned}$$

According to the C-MPC we use the Backward Euler Method to obtain a discretized model with a sampling time equal to 30'.

$$\begin{aligned} x(k+1) &= Ax(k) + Bu(k) + Ew(k) \\ y(k) &= Cx(k). \end{aligned} \tag{5.8}$$

Implicit MPC

The first considered approach is that of the Implicit MPC controller.

The working process of this first version of the MPC can be summarized as

follow:

Algorithm 3 Implicit-MPC

1: build the model for the C-MPC problem;
2: get local measurement (i.e initial state);
3: build weather, occupancy, solar radiation prediction based on a specific criteria;
4: build the constraints and the cost function for the C-MPC over the whole prediction horizon;
5: manage the optimal solution of the C-MPC problem as an input for the T-MPC problem;
6: build the model for the T-MPC problem;
7: construct the constraints and cost function over the whole prediction horizon;;
8: process the optimal solution and actuate them;
9: repeat the whole procedure at the next sampling time.

Certain Equivalence MPC

This is a common practice MPC that simple neglects the uncertainties in the forecast. It takes the imperfect but realistic weather environment prediction and finds its control decision by assuming that this predictions are correct (i.e equal to certain). With respect to this assumption it is possible to formulate the problems associated to the temperature dynamic and the CO_2 concentration.

The CO_2 MPC

The C-MPC problem, at time step t, can then be formulated as:

Problem 12 (Formulation of the MPC for the CO_2 concentration)**.**

$$\min_{u_{CO_2}(t),\dots,u_{CO_2}(t+N-1)} \quad \sum_{k=t}^{t+N-1} u_{CO_2}(k)$$

$$\text{subject to} \quad \begin{aligned} u_{CO_2}^{min}(k) \leq u_{CO_2}(k) \leq u_{CO_2}^{max}(k) \quad & k = t, \dots, t+N-1 \\ 0 \leq y_{CO_2}(k) \leq y_{CO_2}^{max}(k) \quad & k = t, \dots, t+N-1 \end{aligned}$$

where

$$\begin{aligned} u_{CO_2}^{min}(k) &= \dot{m}_{\text{air}}^{\min} \cdot x_{CO_2}(k) \\ u_{CO_2}^{max}(k) &= \dot{m}_{\text{air}}^{\max} \cdot x_{CO_2}(k) \\ y_{CO_2}^{max}(k) &= C_{\text{CO}_2}^{\max} - C_{\text{CO}_2,i} \end{aligned}$$

with N the prediction horizon and $C_{\mathrm{CO_2}}^{\max}$ is equal to the desired upper bound of the CO_2 concentration (e.g. 850ppm).

In Problem 12, at each sampling time, the constraints can be written as:

$$\begin{aligned} g_{u,CO_2}u(k) + g_{x,CO_2}x(k) &\leq b_{CO_2} \\ g_{y,CO_2}y_{CO_2}(k) &\leq b_{CO_2}. \end{aligned} \tag{5.9}$$

where:

$$g_{u,CO_2} = \begin{bmatrix} -1 \\ 1 \end{bmatrix} \qquad g_{y,CO_2} = \begin{bmatrix} -1 \\ 1 \end{bmatrix}$$

$$g_{x,CO_2} = \begin{bmatrix} -1 & 1 \\ 1 & -1 \end{bmatrix} \quad b_{u,CO_2} = \begin{bmatrix} -u_{\min} \\ u_{\max} \end{bmatrix}$$

$$b_y = \begin{bmatrix} -y_{\min} \\ y_{\max} \end{bmatrix}$$

The MPC approach, inherently requires to construct the system dynamic over the whole prediction horizon. This is exploited to obtain at each time step the desired behaviour for the system in an open loop control.
Hence, from the LTI model obtained in the previous section, the state of the system $x_{CO_2}(k)$ after k step is:

$$x_{CO_2}(k) = y_{CO_2}(k) = a^k x_{CO_2 0} + \sum_{i=0}^{k-1} a^{k-i-1} b u_{CO_2}(i) + \sum_{i=0}^{k-1} a^{k-i-1} e w_{CO_2}(i).$$

We can also explicitly define the constraints and the cost function over the whole prediction horizon.

$$\mathbf{U}_{CO_2} = [u_{CO_2}(0), \ldots, u_{CO_2}(N-1)]^T$$

Thus, the Problem 12 can be rewritten compactly:

$$\begin{aligned} \min_{\mathbf{U}_{CO_2}} \quad & ||\mathbf{U}_{CO_2}||_1 \\ \text{subject to} \quad & \mathbf{G}_{u,CO_2}\mathbf{U}_{CO_2} + \mathbf{G}_{x,CO_2} \leq \mathbf{g}_{CO_2} \end{aligned} \tag{5.10}$$

Thanks to the previous model we can derive the matrices to be given to the subsequent CO_2-MPC problem. For the sake of brevity and exposition clarity

we omit to write all the passages in detail. Eventually, the control variable $\dot{m}_{\text{air}}$ can be computed by means of the inverse formula:

$$\dot{m}_{\text{air}}(k) = \frac{u_{CO_2}(k)}{C_{\text{CO}_2}(k) - C_{\text{CO}_2,i}}.$$

The Temperature MPC

The T-MPC problem for the room temperature can be formulated as:

Problem 13 (Formulation of the MPC for the room temperature)**.**

$$\begin{aligned}
\min_{u(t),\ldots,u(t+N-1)} \quad & \textstyle\sum_{k=t}^{t+N-1} c^T u(t) & \\
\text{subject to} \quad & u_{\max} \leq u(k) \leq u_{\min} & k = t, \ldots, t+N-1 \\
& y_{\min} \leq y(k) \leq y_{\max} & k = t+1, \ldots, t+N \\
& T_{\text{air}}^{\min} - T_{\text{room}}(k) \leq \Delta T_h(k) - \Delta T_c(k) \leq T_{\text{air}}^{\max} - T_{\text{room}}(k) & k = t, \ldots, t+N-1 \\
& |\Delta u_h(k) - \Delta u_c(k)| \leq \Delta \dot{m}_{\text{air}}^{\max}(k) |\Delta T_h(k) - \Delta T_c(k)| & k = t, \ldots, t+N-1
\end{aligned}$$

where $\Delta \dot{m}_{\text{air}}^{\max} = \dot{m}_{air}^{\max} - \dot{m}_{\text{air}}^{CO_2}$

Let x_0 denote the current state. It then follows from the linear model (5.8), that the room temperature dynamics over the prediction horizon N can be written as:

$$x(k) = A^k x_0 + \sum_{i=0}^{k-1} A^{k-i-1} B u(i) + \sum_{i=0}^{k-1} A^{k-i-1} E w(i).$$

Operating as for the C-MPC problem, we firstly obtain the description of all the constraints for a fixed time step. Subsequently, we extend the constraints over the whole prediction horizon.

We define:

$$g_u = \begin{bmatrix} -\mathbb{I}_5 \\ \mathbb{I}_5 \end{bmatrix} \qquad g_y = \begin{bmatrix} -\mathbb{I}_2 \\ \mathbb{I}_2 \end{bmatrix}$$

$$g_{u,mixed} = \begin{bmatrix} -1 & 1 & 0 & 0 & 0 \\ 1 & -1 & 0 & 0 & 0 \end{bmatrix} \quad g_{x,mixed} = \begin{bmatrix} -C \\ C \end{bmatrix}$$

$$b_{u,mixed} = \begin{bmatrix} -y_{\min} \\ y_{\max} \end{bmatrix} \qquad b_u = \begin{bmatrix} -u_{\min} \\ u_{\max} \end{bmatrix}$$

$$b_{mixed} = \begin{bmatrix} -T_{\text{air}}^{\min} \\ T_{\text{air}}^{\max} \end{bmatrix}$$

Hence, the constraints can be written:

$$\begin{aligned} g_u u(k) &\leq b_u \\ g_y u(k) &\leq b_y \\ g_{u,mixed} u(k) + g_{x,mixed} x(k) &\leq b_{mixed} \end{aligned}$$

Finally, the whole problem is summarized as follow:

$$\begin{aligned} \min_{\mathbf{U}} \quad & L\mathbf{U} \\ \text{subject to} \quad & \mathbf{G}_u\mathbf{U} \leq \mathbf{b} \end{aligned} \tag{5.11}$$

All the matrices can be found in the Appendix.

Remark: in the C.E approach, the disturbances are treated as a known quantity. This allow, in practice, to obtain linear constraints just on the inputs simply manipulating the constraints with respect to the system dynamic model and the initial state.

Chance Constraints Stochastic MPC (SMPC)

The uncertain nature of environment predictions leads naturally to a probabilistic approach on building control [23]. In particular, this affects the constraints of the problem turning them in the so-called chance constraints. This constraints are in general intractable unless the disturbances follow a specific distribution (e.g Gaussian). This assumption might be rather restrictive hence,

one possibility is to apply a *radomized* method [24]. This approach is briefly described below and it doesn't require to assume a specific distribution for the uncertainties. The method relies just on the capability of randomly extract these uncertainties.

General Chance-constraints formulation : considering the definition given in the previous section, we aim to describe a methodology to tackle a MPC problem in his *chance-constraints* formulation. Once the approach on a generic linear model has been described, the usage in the C-MPC problem or in the T-MPC can be easily derived.
Hence, we consider a generic linear model as:

$$x(k+1) = Ax(k) + Bu(k) + Ew(k)$$

and we obtain the prediction dynamic over the whole prediction horizon. The term x_0 represents, as usual the current measured value of the state and it is thus a known variable.

$$\begin{aligned} \mathbf{x}_N &= \mathbf{A}x_0 + \mathbf{B}\mathbf{u}_N + \mathbf{E}\mathbf{w}_N \\ \mathbf{y}_N &= \mathbf{C}\mathbf{x}_N \end{aligned} \tag{5.12}$$

Regarding the constraints, they can be written in general as:

$$\begin{aligned} \mathbf{V}_{x,mix}\mathbf{x}_N + \mathbf{V}_{u,mix}\mathbf{u}_N &\leq \mathbf{V}_{mix} \\ \mathbf{V}_u\mathbf{u}_N &\leq \mathbf{V}_u \end{aligned} \tag{5.13}$$

Exploiting the (5.12) and substituting in (5.13), it is possible to express all the constraints just as a function of the inputs vector, $\mathbf{u}_N$, and the disturbances vector, $\mathbf{w}_N$.

$$\mathbf{G}_w\mathbf{w}_N + \mathbf{G}_u\mathbf{u}_N \leq \mathbf{g} \tag{5.14}$$

We remark that the disturbances vector, over the prediction horizon, can be thought as a generic uncertain vector that, depending on the circumstance, can incorporate either just the occupancy (C-MPC), that also weather and solar radiation prediction (T-MPC).

The *chanche constraints* method relax the constraints in (5.14) contemplating a possible violation with a probability that is less of a predefined

level.

$$\mathbb{P}\left[\mathbf{G}_u\mathbf{u}_N + \mathbf{G}_w\mathbf{w}_N \leq \mathbf{g}\right] \geq 1 - \alpha \tag{5.15}$$

with $\alpha \in [0, 1]$ being the violation probability level. In this approach, the parameter α represents the trade-off between energy performances and comfort. Control designer's task is to calibrate its value in order to achieve the best results.

As previously said, chance constraints are not easy to handle since they require multi-dimensional integrations and can lead to non-convex admissible set. A possible conservative solution is to build a scenario-based [2] approximation approach.

Scenario-based approach We aim to substitute the constraints in (5.14) with a set of deterministic constraints.
The algorithm can be summarized as follow:

1. create a set of S i.i.d. disturbances samples, $\mathbf{w}^1, \ldots, \mathbf{w}^S$. Each of them is a reasonable disturbance for the studied problem over the whole prediction horizon.

2. replace the chance constraints with S deterministic constraints

$$\mathbf{G}_u\mathbf{u}_N + \mathbf{G}_w\mathbf{w}_N^i \leq \mathbf{g} \quad i = 1, \ldots, S$$

3. reduce the complexity of the problem cutting redundant constraints. Hence, among the S constraints, just one really affects the feasible set.

$$\mathbf{G}_u\mathbf{u}_N \leq \mathbf{g} - \max_{i=1,\ldots,S} \mathbf{G}_w\mathbf{w}_N^i$$

4. soften the obtained constraints in order to guarantee feasibility [3]

$$\mathbf{G}_u\mathbf{u}_N \leq \mathbf{g} + \epsilon - \max_{i=1,\ldots,S} \mathbf{G}_w\mathbf{w}_N^i$$

where ϵ is a vector of N elements (MISO system) often called the slack variables vector.

[2] Scenarios are defined as i.i.d. samples of a random vector.

[3] It has to be noticed that this approach may be highly conservative and lead to infeasible problem since it requires to satisfy the constraints in the most disadvantageous case.

We can finally formulate the general problem for the SMPC.

Problem 14 (General SMPC formulation)**.**

$$\begin{aligned} &\min_{\mathbf{u}_N} \quad \mathbf{c}^T\mathbf{u}_N + \rho\mathbf{1}^T\epsilon \\ &\text{subj.to} \quad \mathbf{G}_u\mathbf{u}_N \leq \mathbf{g} + \epsilon - \max_{i=1,\dots,S} \mathbf{G}_w\mathbf{w}^i \end{aligned}$$

where :

- $\mathbf{c}^T$ is the linear cost matrix accounting for the energy use over the whole prediction horizon;
- $\mathbf{1}$ is a matrix containing ones with appropriate dimensions.

,

The number of Scenarios in 14 has to be chosen in order to assure a feasible solution for the SMPC problem. A sufficient condition guarantee this and it is given by the following expression [24]:

$$S \geq \frac{2}{\alpha}\left(\ln\frac{1}{\beta} + d\right) \tag{5.16}$$

with d the number of decision variables in the formulated problem [4], and β a parameter called, *confident parameter* that has to be set by the user. If, for instance, we consider $\alpha = 0.1$ and $\beta = 0.001$ which means that we choose a confident level of 99% and a constraint satisfaction probability level of 90%. With respect to these values we obtain a required minimum number of scenarios equal to 5500. We now want to study the actual sensitivity on the number of extracted samples of the performance of the SMPC (in terms of energy use and violations of the thermal comfort levels). To this aim we simulate the energy use and the energy use and the amount of violations of thermal comfort corresponding to a number of scenarios varying from 10 to 5500.

In these simulations we use historical data, and thus consider a specific day in March 2014, for which we measured an occupancy pattern of 3-5 people always present in the room, except during early morning and lunch time. We can notice that all the simulated T-SMPC controllers yield to similar violation frequencies, although the energy use for the cases of 4000 and 5500 is higher,

[4] If we consider a problem with $u(k) \in \mathbb{R}^m$, $\epsilon(k) \in \mathbb{R}^p$, and N as the prediction horizon, then $d = (p+m)N$

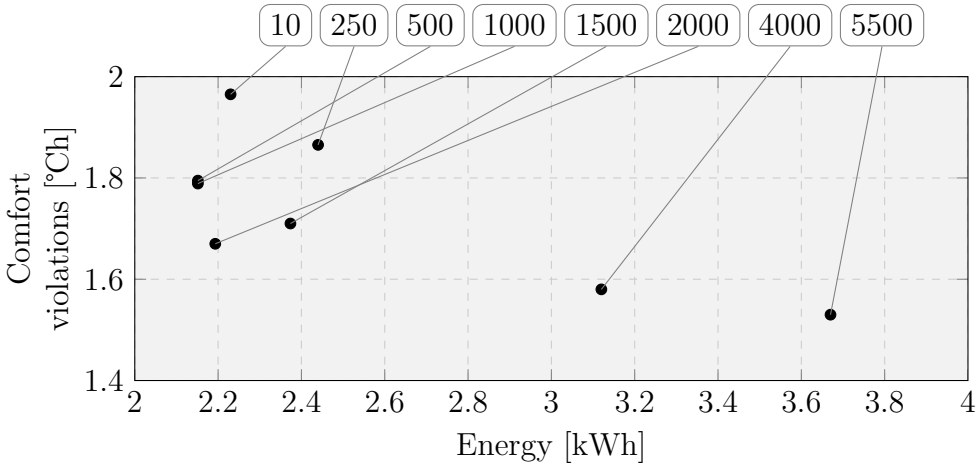

Figure 5.2: Temperature violations vs energy use for T-SMPC for various number of scenarios.

due to the fact that these high numbers introduce greater conservatism. In terms of violation probability, the unique T-SMPC controller that does not fulfil the probability constraints is the one with 10 scenarios, since the corresponding violation probability is greater than 10%. In this specific simulation case, 250 scenarios are enough to keep the desired violation probability. With this simulation study we thus confirm the general finding that the theoretical bound in 5.16 tends to be over pessimistic. This is mainly due to the conservatism introduced by the scenario-based approach and due to the feedback mechanism, which yields less violations compared to open-loop approaches.

The last thing to specify is the extracting scenarios process. This is conducted exploiting a probabilistic tool known as *copulas*. Copula is a function $\mathbb{C} : [0,1]^N \mapsto [0,1]$ that allow to re-write the Cumulative Distribution Function (CDF) of of any S-uple of random vector $w_1, \ldots, w_S$ in terms of the marginal distribution. In this way, it is possible to reconstruct the CDF simply reconstructing a marginal distribution and this function $\mathbb{C}(\cdot)$.
The learning of the copula from real data and the actual implementation of this tool is beyond the scope of this thesis. For further details the reader is referred to [23].

Explicit MPC

In this section we present the explicit formulation of our specific case study. With respect to the simplified model for the thermal dynamic 3.9, we now aim

to compute the partition of the state space, as well as the PWA function, to evaluate the control inputs.
Since the main goal of this new approach is to reduce the on-line computational time, we just focus on the scenario-based approach that is the most time demanding scheme. We remark that the formulation for the problem in the explicit version is entirely equivalent to the one explained in the previous section, the sole difference relies on the fact that the explicit MPC uses the simplified model for the thermal dynamic.
the results we present have been obtained exploiting the Matlab toolbox MPT.

We remind that the problem formulation of the specific case study requires to solve firstly the problem related to the IAQ (5.10). The obtained optimal input (i.e m_{air}), is passed to the problem for the indoor temperature as a lower bound to the ventilation. This assumption reflects the fact that, in general, the quality of air (i.e the concentration of the CO_2) is a more important parameter with respect to the thermal comfort.

Thus, from the previous discussion, we firstly obtain the partition of the state space and the PWA map for CO_2 problem.
In particular, we focus on the chance constraints stochastic approach explained in Section 5.2. Since the computation is performed off-line, we decided to focus on the period of time between 8.00 am and 8.00 pm. This choice affects both the generation of the scenarios, and also the considered bounds for actuation [5].
The obtained results are depicted in Figure 5.3.

The different colours refer to different regions of the state space. Every region is associated with a different piecewise affine function of the initial state. In the CO_2 problem, since the state space is mono-dimensional, the PWA functions are simply straight lines with different slopes.
We now need to traduce the value of u_{CO_2} in the correspondent value for $\dot{m}_{\text{air}}(k)$. That can be done as previously explained as follows:

$$\dot{m}_{\text{air}}(k) = \frac{u_{CO_2}(k)}{C_{\text{CO}_2}(k) - C_{\text{CO}_2,i}} \tag{5.17}$$

The next step is to traduce the information coming from the CO_2 problem in a lower bound for the temperature problem. We remark that, since the computation is performed off-line, the lower bound, $\dot{m}_{CO_2}$, for the temperature

[5] We remind that the ventilation and the cooling processes can be actually performed when the central fan is running.

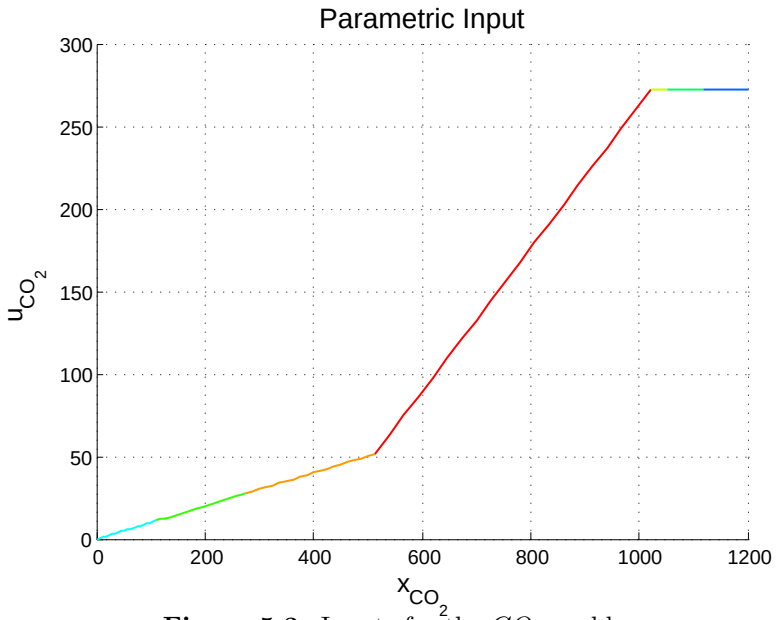

Figure 5.3: Inputs for the CO_2 problem.

problem has to be set in the problem formulation. Thus, for each value of $\dot{m}_{CO_2}$ a different problem for the thermal dynamics is associated.
The problem we have to face is how to partition the values of $\dot{m}_{CO_2}$ in order to obtain a finite, not too large, numbers of possible temperature problem.

First of all, considering the slopes in Figure 5.3 we notice that, among all the computed regions, just three of them are actually significant. Given that

Region	$x_{\mathrm{CO_2}}$	$u_{\mathrm{CO_2}}(x_{\mathrm{CO_2}})$	$\dot{m}_{\mathrm{air}}$	A_{v}
$\mathcal{R}_1$	$[0, 513]$	$0.099x_{\mathrm{CO_2}}$	$[0, 0.099]$	[0 %, 18.78%]
$\mathcal{R}_2$	$[513, 1022]$	$0.443x_{\mathrm{CO_2}} - 176.379$	$[0.099, 0.27]$	[18.78 %, 100%]
$\mathcal{R}_3$	$[1022, 1200]$	276.367	$[0.23, 0.27]$	[98 %, 100%]

Table 5.1: Reduction of the partition for the state space.

relationship between $\dot{m_{\mathrm{air}}}$ and A_v, and then to consider increments of less than 5% would result in negligible changes in practice ventilation for the ventilation. In particular, we divide the possible values for the lower bound $\dot{m_{\mathrm{air}}}$ in intervals which correspond to increments of 5 % on the opening valve, A_v. From the Figure 5.4, we notice that actually not all the values of A_v are acceptable since they require a value for $\dot{m_{\mathrm{air}}}$ that is inferior with respect to the minimum one [6]. Eventually we obtained 16 different lower bound for the temperature problem.

[6] In the analysis of the ventilations system it has been identified how the values of $\dot{m_{\mathrm{air}}}$ can actually ranges in $[0.1002, 0.278]$

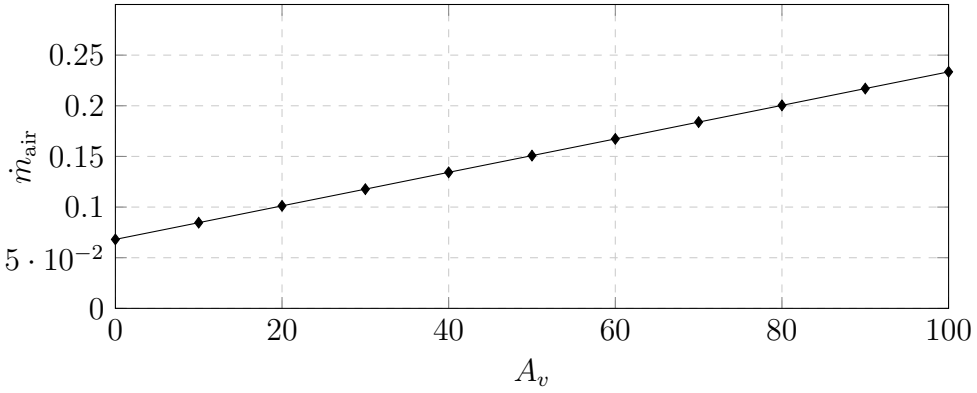

Figure 5.4: Map for the conversion between the valve opening percentage and the mass air flowing into the room.

By setting, for instance, $\dot{m_{\text{air}}} = 0.1001$ an instance for the problem of temperature is obtained. The parametric inputs related to this particular problem are depicted in Figures (5.5, 5.6, 5.7, 5.8). We notice that the heating process related to the ventilation unit is identically equal to zero since it requires more energy with respect to the heating related to radiators. Moreover, the heating additional power Δu_h is not reported since, from the problem formulation 13, having ΔT_h identically equals to zero forces Δu_h to be zero as well.

We finally introduce the procedure related to the Explicit MPC in our specific case study.

Algorithm 4 Explicit-MPC

1: get local measurement (i.e initial state);
2: evaluate the PWA function for the CO_2 problem obtaining $\dot{m}_{\text{air}}$;
3: identify the membership of $\dot{m}_{\text{air}}$ to one of the possible clustered regions;
4: select the corresponding PWA function for the temperature problem;
5: evaluate the PWA function with respect to the current state obtaining the inputs;
6: process the optimal solution and actuate them;
7: repeat the whole procedure at the next sampling time.

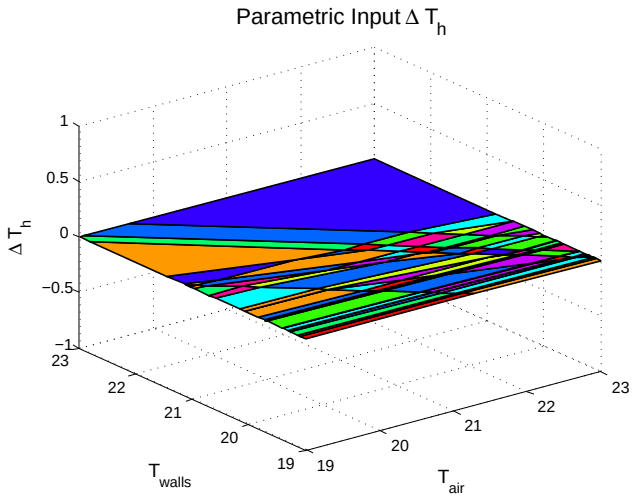

Figure 5.5: PWA function to evaluate ΔT_{heat} with respect to the initial state x_0

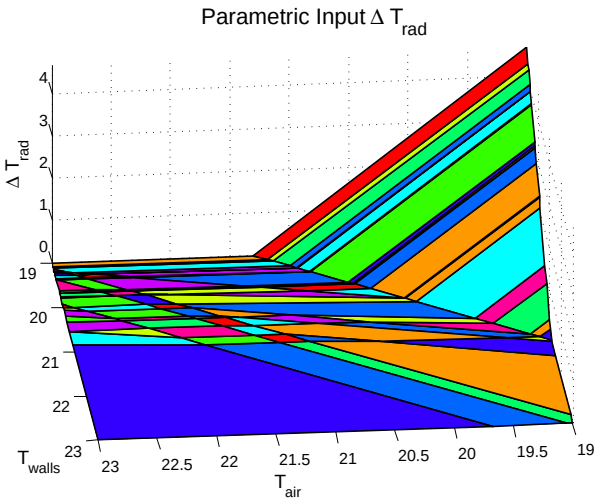

Figure 5.6: PWA function to evaluate ΔT_{r} with respect to the initial state x_0

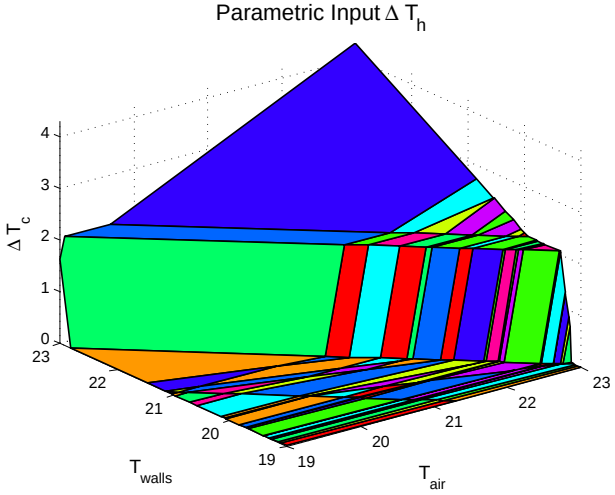

Figure 5.7: PWA function to evaluate ΔT_{cool} with respect to the initial state x_0

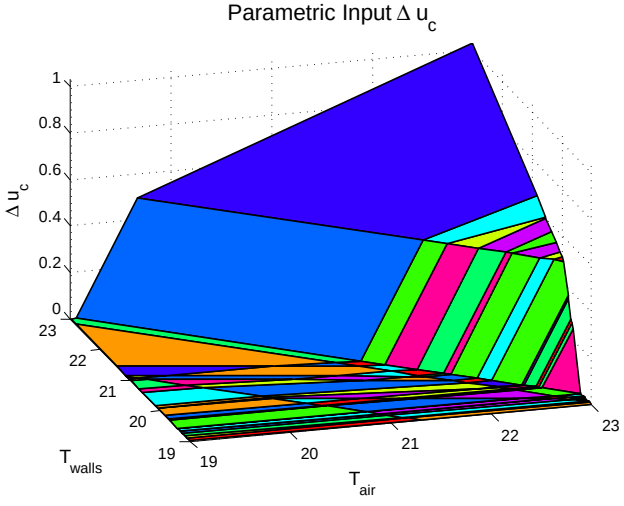

Figure 5.8: PWA function to evaluate $\Delta_u \text{co}$ with respect to the initial state x_0

5.3 Post processing

The values obtained from one of the previous MPC at each sampling time can not be directly used to command the actuators. Indeed the assumptions made in Section 5.2, stating that the problems can be reduced to linear optimization problems, must be modified to account for the peculiarities of the hardware in the testbed. Our choice is to exploit a post-processing phase that transforms the information coming from the two problems, T-MPC and C-MPC, into signals that correspond to how much the various valves of the plant should be open.

Consider then that the information coming from the T-MPC is composed by ΔT_h ΔT_c Δu_h, Δu_c, ΔT_{mr}. From the CO_2 - MPC instead provides $\dot{m}_{\text{air}}^{CO_2}$, the lower bound on the air flow rate. The following Algorithm 5 reports this transformation procedure. We now comment Algorithm 5. The first part of the algorithm performs an analysis on the validity of the solution. In particular it takes care of removing non-optimal solutions in which both cooling and heating system are activated. This condition can arise, for instance, to assure feasibility to the problem in absence of the soft constraints.

Afterwards the procedure examines the optimal and valid solution obtaining the values of the actuations by means of simple arithmetic operations. All these operations derive directly from the definitions of the models used to set the MPC-problems.
The formula at row 23 is an heuristic identified formula that is used to obtain the temperature required to the air conditioning, T_{sa} system in order to assure a total temperature flowing the ventilation system equal to T_{air}. That is:

$$\Delta T_c = \dot{m}_{\text{air}}\big(T_{\text{room}} - T_{\text{air}}\big) = \dot{m}_{\text{air}}\big(T_{\text{room}} - 0.68T_{\text{ai}} - 0.32T_{\text{sa}}\big)\,, \tag{5.18}$$

The set points obtained through the high-level MPC controller, and the post-processing phase, are then actuated via low-level PI controllers that regulate valve opening percentage of the ventilation, cooling, and heating system.

Eventually, the overall functioning of the KTH-HVAC system is depicted in Figure 5.9 for the Implicit MPC, and in Figure 5.10.

Algorithm 5 Post-processing

Require: ΔT_h, ΔT_c, Δu_h, Δu_c, ΔT_{mr}, $\dot{m}_{\text{air}}^{CO_2}$
Ensure: T_{sa}, T_{mr}, $\dot{m}_{air}$

if $\Delta T_h \geq 0$ and $\Delta T_c \geq 0$ **then**
    if $\Delta T_c \geq \Delta T_h$ **then**
        $\Delta T_c = \Delta T_c - \Delta T_h$
        $\Delta T_h = 0$
    else
        $\Delta T_h = \Delta T_h - \Delta T_c$
        $\Delta T_c = 0$
if $\Delta u_h \geq 0$ and $\Delta u_c \geq 0$ **then**
    if $\Delta u_c \geq \Delta u_h$ **then**
        $\Delta u_c = \Delta u_c - \Delta u_h$
        $\Delta u_h = 0$
    else
        $\Delta u_h = \Delta u_h - \Delta u_c$
        $\Delta u_c = 0$
$T_{sa} = 0$
$T_{mr} = 0$
$\dot{m}_{\text{air}} = \dot{m}_{\text{air}}^{CO2}$
if $\Delta T_h > 0$ **then**
    if $\Delta u_h > 0$ **then**
        $\dot{m}_{\text{air}} = \dot{m}_{\text{air}} + \frac{\Delta u_h}{\Delta T_h}$
if $\Delta T_c > 0$ **then**
    $T_{air} = T_{\text{room}} - \Delta T_{\text{cool}}$
    $T_{sa} = \frac{T_{air} - 0.68 T_{ai}}{0.32}$
if $\Delta u_c > 0$ **then**
    $\dot{m}_{\text{air}} = \dot{m}_{\text{air}} + \frac{\Delta u_c}{\Delta T_c}$
if $\Delta T_{rad} > 0$ **then**
    $T_{mr} = T_{room} + \Delta T_{rad}$

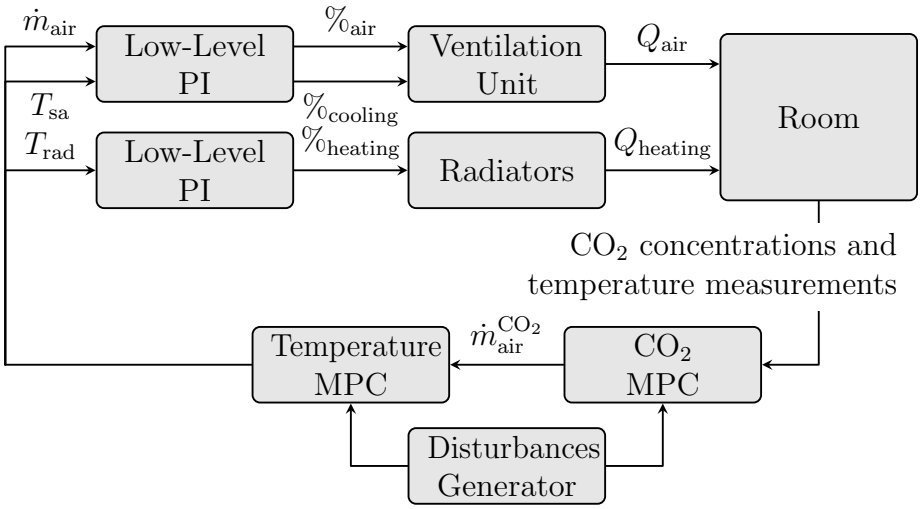

Figure 5.9: Schematic of the whole KTH-HVAC system with Implicit MPC.

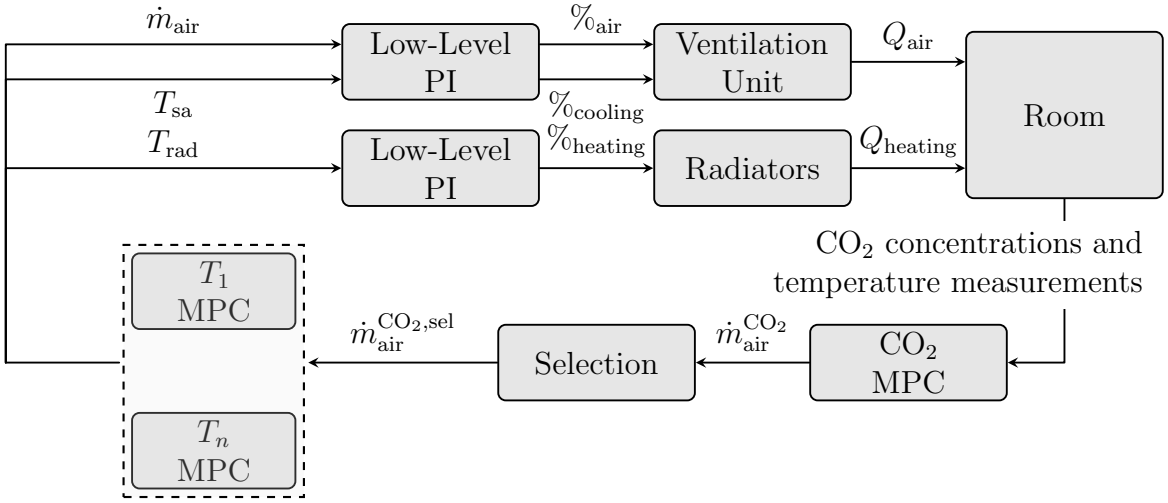

Figure 5.10: Schematic of the whole KTH-HVAC system with Explicit MPC.

5.4 Energy Indices

A crucial aspect to consider, when it comes to analyze and study the behaviours of a controller, is that of the performance indices. The aim of this section is that of introducing simple parameters in order to evaluate the implemented controllers.
We remind that our goal is to assure thermal comfort and quality of air, while minimizing the energy consumed to meet these requirements. Hence, the chosen indices are:

- total energy usage for actuations. We obtained numerical values that quantify approximately the actual energy spent by the heating, cooling and venting systems.
- levels of violations of thermal comfort bound expressed in degree/hours.

The trade off between the two goals can be tuned adjusting the control parameters that characterize the different controllers. In the following, we present the procedure to evaluate the aforementioned indices.

Algorithm 6 Indices Evaluation

Require: $\dot{m}_{\text{air}}(k)$, $T_{\text{sa}}(k)$, $T_{\text{mr}}(k)$, N
Ensure: E_{tot}, C_{viol}
for i=1:N **do**
  if $\dot{m}_{\text{air}}(i) > 0$ **then**
    if $T_{\text{sa}}(i) > 0$ **then**
      $E_{\text{vent}} = E_{\text{vent}} + ||1006 \cdot 0.68 \cdot \dot{m}_{\text{air}}(T_{\text{ai}}(i) - T_{\text{room}}(i))||\Delta t$
      $E_{\text{cool}} = E_{\text{cool}} + ||1006 \cdot 0.32 \cdot \dot{m}_{\text{air}}(T_{\text{sa}}(i) - T_{\text{room}}(i))||\Delta t$
    else
      $E_{\text{vent}} = E_{\text{vent}} + ||1006 \cdot \dot{m}_{\text{air}}(T_{\text{ai}}(i) - T_{\text{room}}(i))||\Delta t$
  if $T_{\text{mr}} > 0$ **then**
    $E_{\text{heat}} = E_{\text{heat}} + A_{\text{rad}} \cdot h_{\text{rad}}(T_{\text{ai}}(i) - T_{\text{room}}(i))\Delta t$
  if $T_{\text{room}} > T_{\text{room}}^{\max}$ **then**
    $C_{\text{viol}} = C_{\text{viol}} + (T_{\text{room}}^{\max} - T_{\text{room}})\Delta t$
  else
    if $T_{\text{room}} < T_{\text{room}}^{\min}$ **then**
      $C_{\text{viol}} = C_{\text{viol}} + (T_{\text{room}} - T_{\text{room}}^{\min})\Delta t$
$E_{\text{tot}} = E_{\text{vent}} + E_{\text{cool}} + E_{\text{heat}}$

The procedure simply evaluate the energy consumption from the registered actuation values weighing for terms that indicate the related cost. Moreover, this value is integrated for the length of the time interval.

6 Results

6.1 Numerical Results

In this section we discuss some numerical experiments. In particular, we aim to compare the behaviour, with respect to the performances indices introduced in the previous section, for:

- **I-CE**: the Certain Equivalence version of the Implicit MPC controller;
- **I-SMPC**: the Scenario-Based version of the Implicit MPC controller;
- **E-SMPC**: the Scenario-Based version of the Explicit MPC controller.

Moreover, we take as an ideal reference for the simulation case, the so-called *Performance Bound* MPC **(PB)**.
The Performance Bound MPC is a particular controller which has perfect knowledge of the control system's dynamic as well as perfect knowledge of all future disturbances acting upon the system. This controller exploits all these information to obtain the optimal control profile with respect the defined cost function. Hence, the PB represents an absolute benchmark for all the possible controller related to the same optimization target, all performances of

other controllers will be worse. For the sake of clarity in the visualization of the results, we only report what has been obtained for (I-CE) only in terms of performances without showing all the actuations, the thermal dynamic, and the dynamic of the air inside the room. This allows to focus more just on the comparison between I-SMPC and E-SMPC and to analyze deeply the differences between them.

In our simulation we identify the real plant with the identified model in (3.17) for the CO_2 dynamic, and the 13-states model for the thermal dynamic. This assumption implies, as a direct consequence, that the model error is equal to zero for the Implicit MPC. The only source of uncertainty for the Implicit MPC is then represented by random disturbances acting on the system. In particular, these disturbances are taken from real measured data retrieved in the testbed throughout the deployed sensors.

We report three simulations corresponding to three different scenarios for the disturbances:

- **Test 1**:
  - winter scenario for the outside temperature;
  - peak for occupancy = 8 people;
  - $T_{air} \in [20, 22]$;
  - CO_2 bounded under 850 ppm;
  - Period = 12 h, form 8am to 8pm.

  The results are shown in Figure 6.1 at page 78

- **Test 2**:
  - winter scenario for the outside temperature;
  - peak for occupancy = 2 people;
  - $T_{air} \in [20, 22]$;
  - CO_2 bounded under 850 ppm;
  - Period = 12 h, form 8am to 8pm.

  The results are shown in Figure 6.2 at page 79

- **Test 3**:
  - summer scenario for the outside temperature ;
  - peak for occupancy = 6 people;
  - $T_{air} \in [20, 22]$;
  - CO_2 bounded under 850 ppm;
  - Period = 12 h, form 8am to 8pm.

  The results are shown in Figure 6.2 at page 80

All the simulation we conducted, show the effectiveness of the explicit controller. In fact, analyzing the figures that show the performance of the three controllers, and comparing with the trends of temperature and quality of air, it is clear how the explicit controller is able to ensure compliance with the limits on the comfort inside the room. Furthermore, its performance is comparable in term of energy consumption with respect to the implicit MPC controller.

We want to point out that a large quantity of simulations were carried out trying to investigate how the various parameters involved could afflict the comparison between the two controllers. The results we obtained have shown that the overall behavior is qualitatively independent of these parameters. As a further confirmation of this fact we report the performance evaluations obtained by varying the disturbances acting on the system (Figure 6.7 at page 82). So the selected simulations can be taken as significant examples for the comparison between the two controllers.

Observing the previous figures, we can conclude that, in general, the I-SMPC slightly outperforms the E-SMPC. This is due to the fact that E-SMPC exploits a simplified model to obtain the control profile. The approximations inherently related to the two-states, with respect to the more complex 13-states, can affect the quality of the predictions for the optimization problem and so the results in terms of performance.

In all the Figures (6.4, 6.5, 6.6), the performance of the Certain Equivalence controller are reported. As expected, they show both high levels of energy spent for the actuations and a high value of thermal violations in the analyzed time period. This is due to the fact that it does not take into account the inherent uncertainty related to disturbances acting on the system.

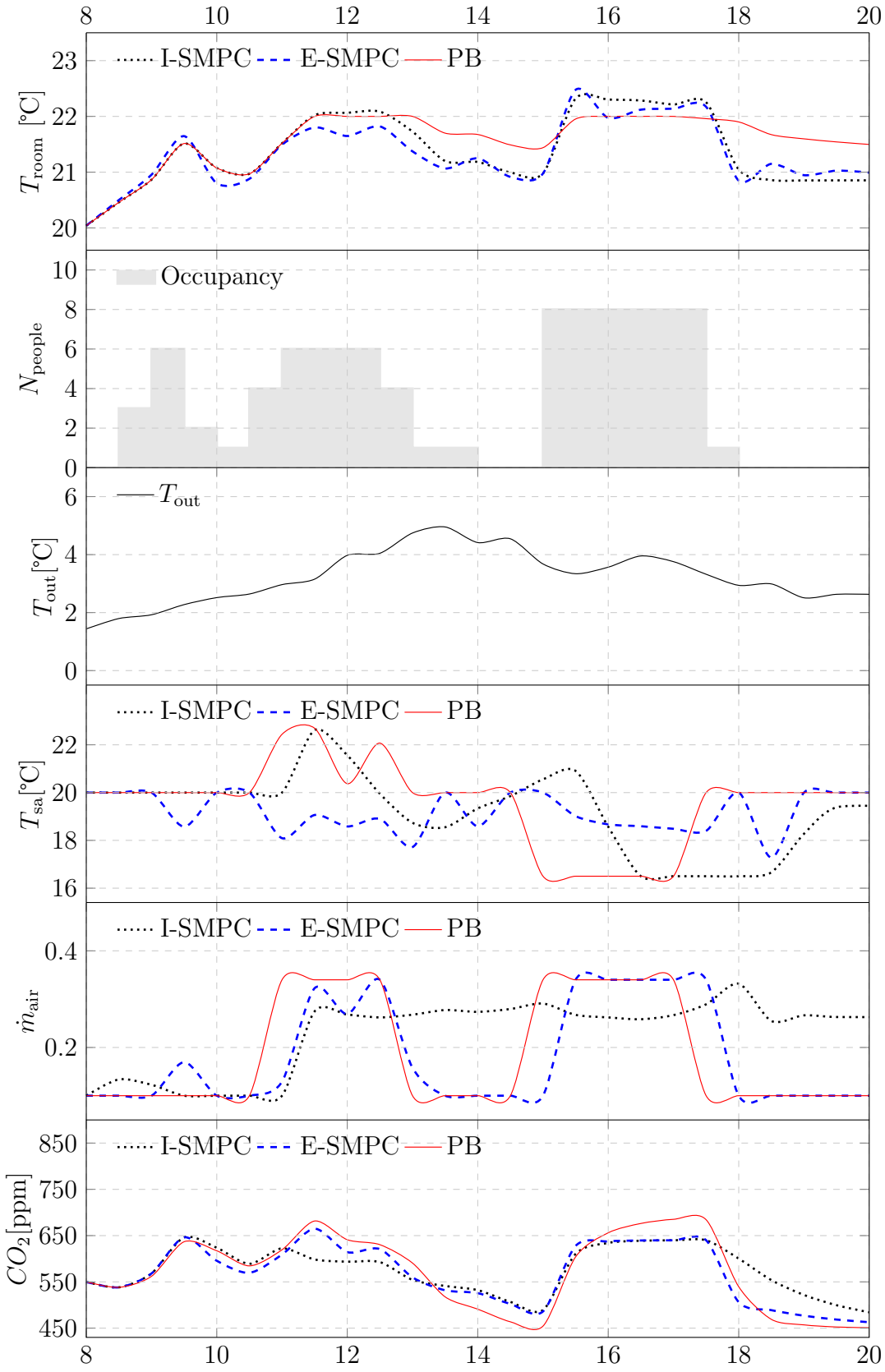

Figure 6.1: Simulation 1 on the MPCs: cooling action, high occupancy, winter. The temperature comfort bounds are set to 20 ℃ to 22 ℃ while the upper bound of the CO_2 concentration is 850 ppm.

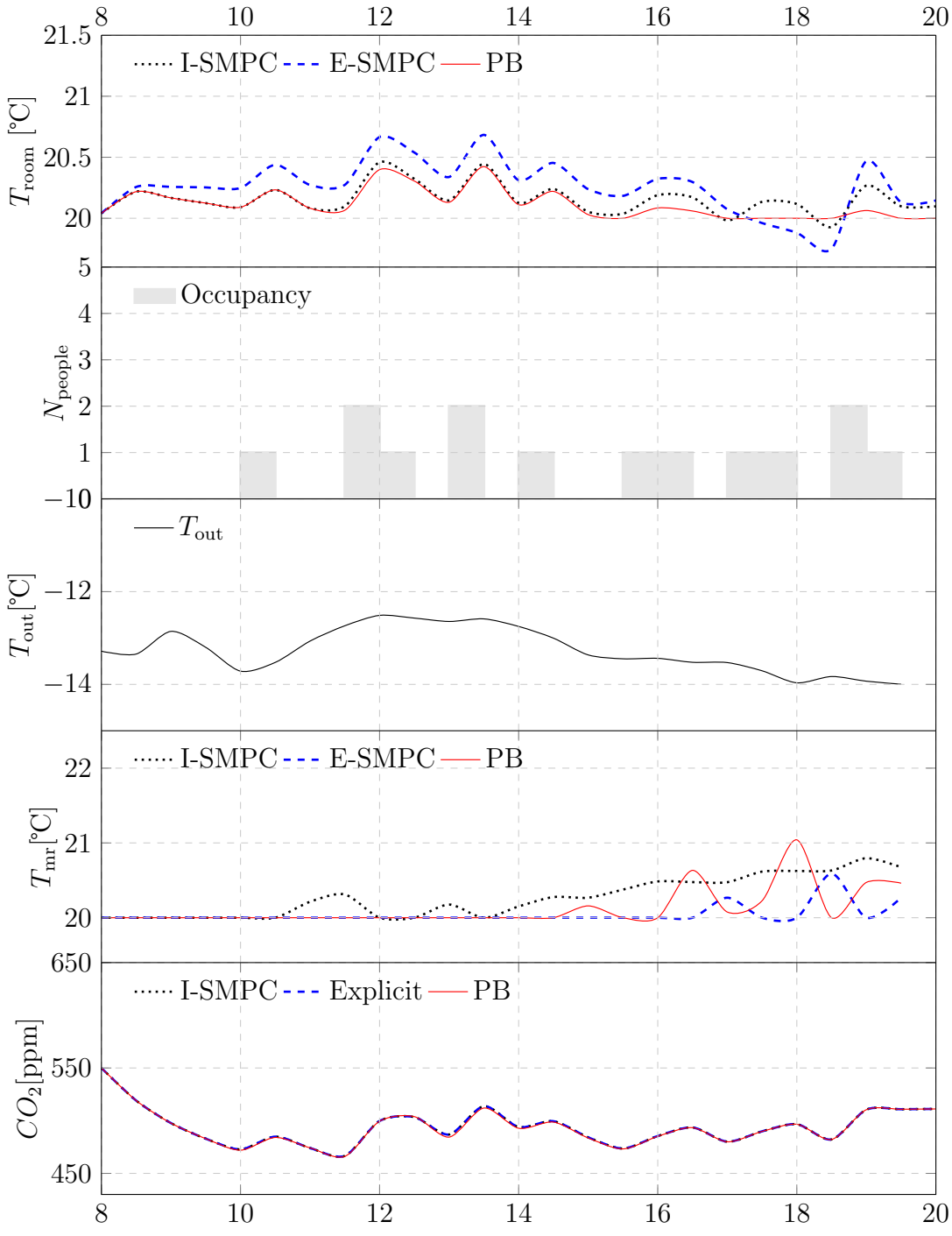

Figure 6.2: Simulation 2 on the MPCs: heating action, low occupancy, winter. The temperature comfort bounds are set to 20 °C to 22 °C while the upper bound of the CO_2 concentration is 850 ppm.

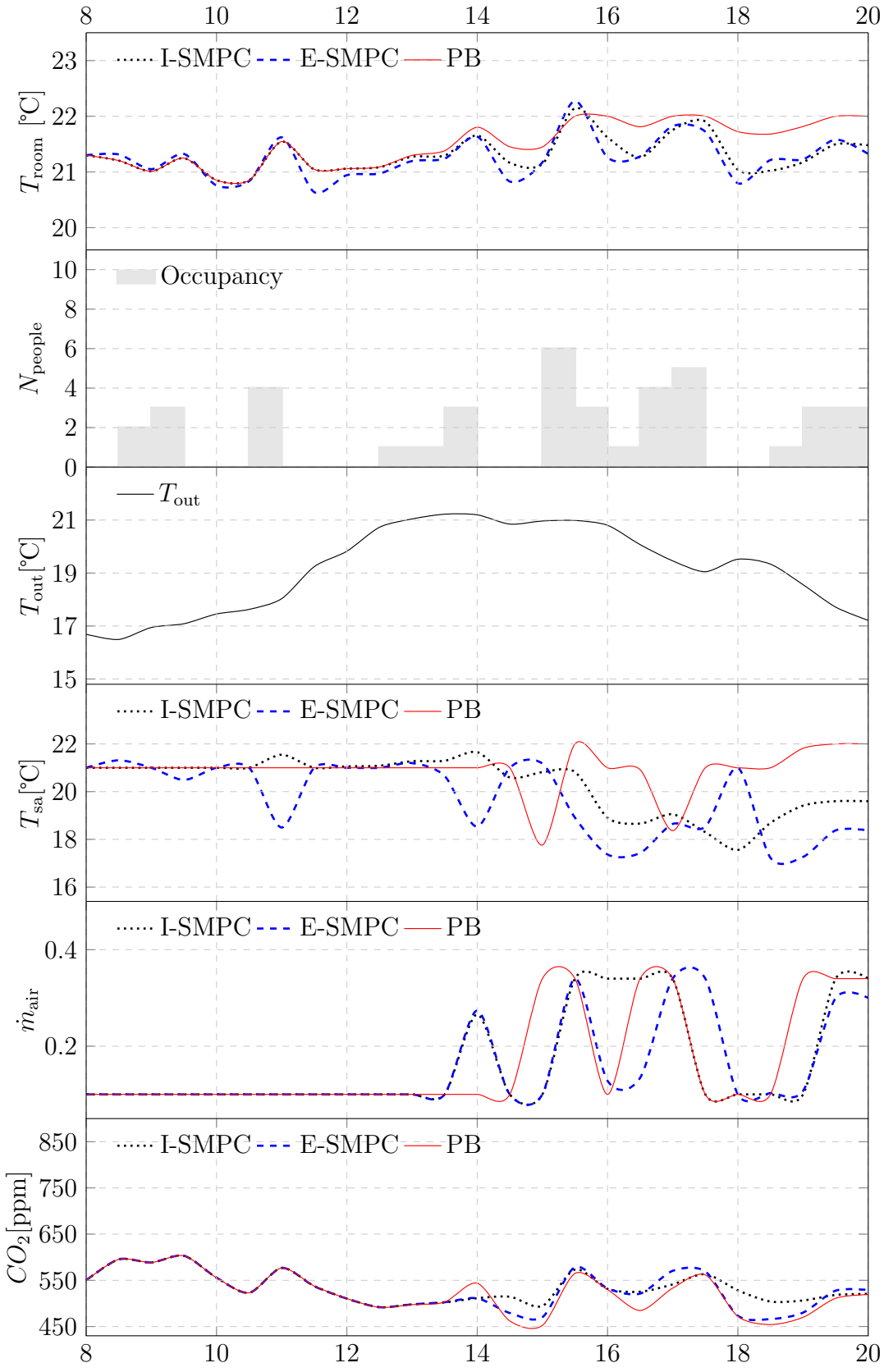

Figure 6.3: Simulation 3 on the MPCs: cooling action, average occupancy, summer. The temperature comfort bounds are set to 20 ℃ to 22 ℃ while the upper bound of the CO_2 concentration is 850 ppm.

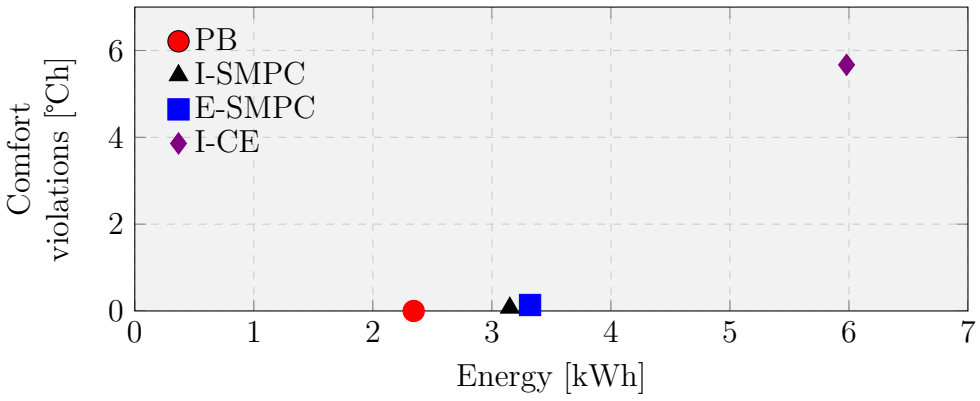

Figure 6.4: Performances for the simulation 1 on the MPCs: cooling action, high occupancy, winter.

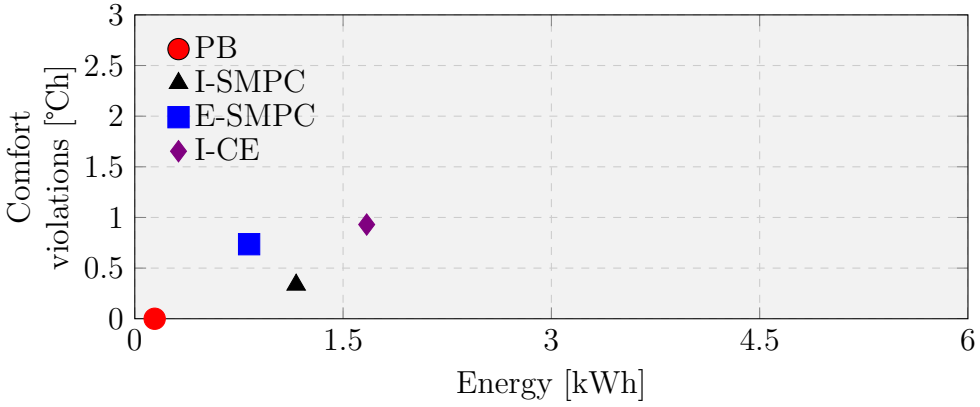

Figure 6.5: Performances for the simulation 2 on the MPCs: heating action, low occupancy, winter.

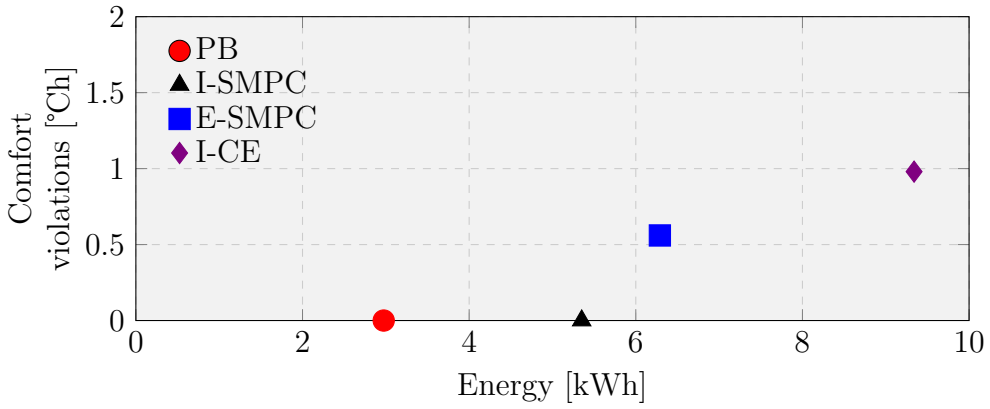

Figure 6.6: Performances for the simulation 3 on the MPCs: cooling action, low occupancy, summer.

We remark that violations for CO_2 are not taken into account in the performances evaluations. This is because of the fact that, in general, thermal constraints require the activation of the ventilation system ensuring that CO_2 never reaches the alert level. So in all the simulations we conducted, we never detect violations on bound for the quality of air. For instance, Simulation 1 considers a case with very high occupancy, meaning thus an high CO_2 production rate. Also in this case the temperature problem, in order to decrease the temperature, provides an additional boost to $\dot{m}_{\text{air}}$ helping to decrease the CO_2.

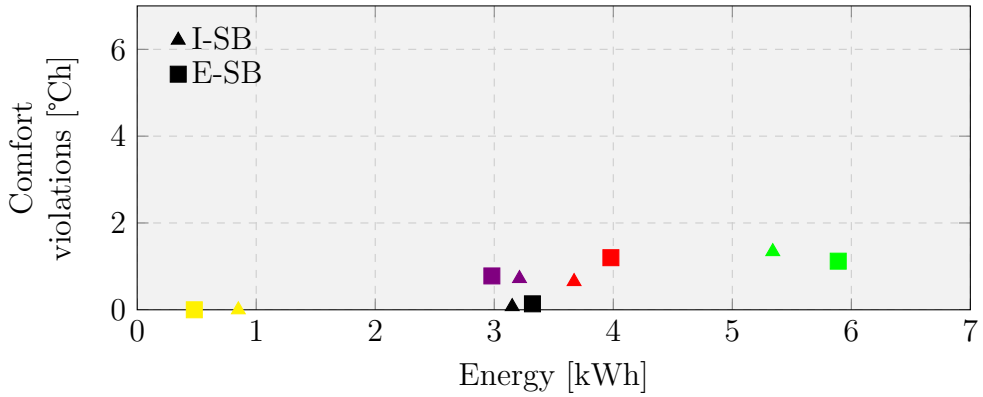

Figure 6.7: Comparison between implicit and explicit MPC with respect to different disturbances acting on the system.

6.2 Experimetal Results

In the previous section we have shown the tractability of the explicit MPC control approach to HVAC system, at least from the point of view of numerical simulation. We now aim to present the results that we obtained applying our controller to the testbed. We just focus on the explicit SMPC controller and we remind the reader to [22] for experiments on the implicit SMPC controller. In order to have a reference in the evaluation of the performance of our controller, we compare two two different controllers:

- **AHC**: the current practice presented in Chapter 4, a simple control logic with PIC control loops and switching logic;
- **E-SMPC**: the Scenario-Based version of the Explicit MPC controller.

For the E-SMPC we consider a prediction horizon of 9 hours and a sampling time of 10 minutes, hence that we have a number of prediction steps equal to $N = 54$. The optimal control laws have been computed with Matlab on an Intel(R) Core(TM)i7-2600 CPU,3.40 GHz and 8Gb of RAM. The average amount of time needed to compute the optimal solutions was 20 minutes, obtaining a PWA function consisting of 800 polyhedra in the set of admissible initial conditions. As well as for the numerical results, we aim at testing the performance of our E-SMPC in terms of energy use and comfort as well as the effect of a different number of scenarios in real experiments. Hence, we conducted three different tests in March 2014.

- **E-SMPC**, 18-3-2014:
  - 10 scenarios;
  - peak for occupancy = 3 people;
  - $T_{air} \in [20, 22]$;
  - CO_2 bounded under 850 ppm;
  - Period = 9 h, form 7.00 to 16.00.

  The results are shown in Figure 6.1 at page 85

- **AHC**, 19-3-2014:
  - peak for occupancy = 4 people;
  - $T_{air} \in [20, 22]$;
  - CO_2 bounded under 850 ppm;
  - Period = 9 h, form 7.00 to 16.00.

  The results are shown in Figure 6.8 at page 85

- **E-SMPC**, 20-3-2014:
  - 1000 scenarios ;
  - peak for occupancy = 8 people;

- $T_{air} \in [20, 22]$;
- CO_2 bounded under 850 ppm;
- Period = 9 h, form 7.00 to 16.00.

The results are shown in Figure 6.9 at page 86

We then compare the AHC with E-SMPC with 10 scenarios in Test 1 and with E-SMPC with 1000 scenarios in Test 2. Each row of Figure 6.8 depicts the disturbances (i.e., outdoor temperature and occupancy), the control inputs (i.e., supply air temperature and massflow) and the controlled indoor temperature and CO_2 levels. The horizontal axis reports the time period of the experiments, from 7:00 to 16:00. Despite the cold season, both controllers in both tests require cooling when there is people in the room. The demand for cooling during the cold season can be explained by the relatively high internal gains, due to occupancy and equipment, and by the limited and moderately insulated external walls surface. This implies that the thermal indoor dynamics are significantly affected by the occupancy patterns.

Notice that on the 18th and on the 20th, the days when the E-SMPC was applied, both the outdoor temperature and the occupancy was higher compared to the day when AHC was employed. In particular, the occupancy was significantly higher on the 20th, after lunch time. Despite these more challenging disturbances, the temperature profiles resulting from the E-SMPC are very similar to the ones obtained by AHC. The E-SMPC is capable to keep the temperature profile close to the upper bound, although the E-SMPC with 10 scenarios violated this bound more often.

Despite the temperature profiles resulting form the two controllers being indeed close, the E-SMPC achieved this result at a significant lower energy cost. This is a promising performance, especially considering the higher occupancy and outdoor temperatures that the E-SMPC needed to compensate. This can be clearly seen by looking at the required massflow in : the AHC turns on/off the cooling system quite often, while the E-SMPC uses the cooling system fewer times, i.e., only when really convenient.

Numerically, for the E-SMPC $E_{\text{tot}} = 0.77$kWh on the 20th, and $E_{\text{tot}} = 0.79$kWh on the 18th, while for the AHC $E_{\text{tot}} = 1.04$kWh, approximatively $31 - 33\%$ higher.

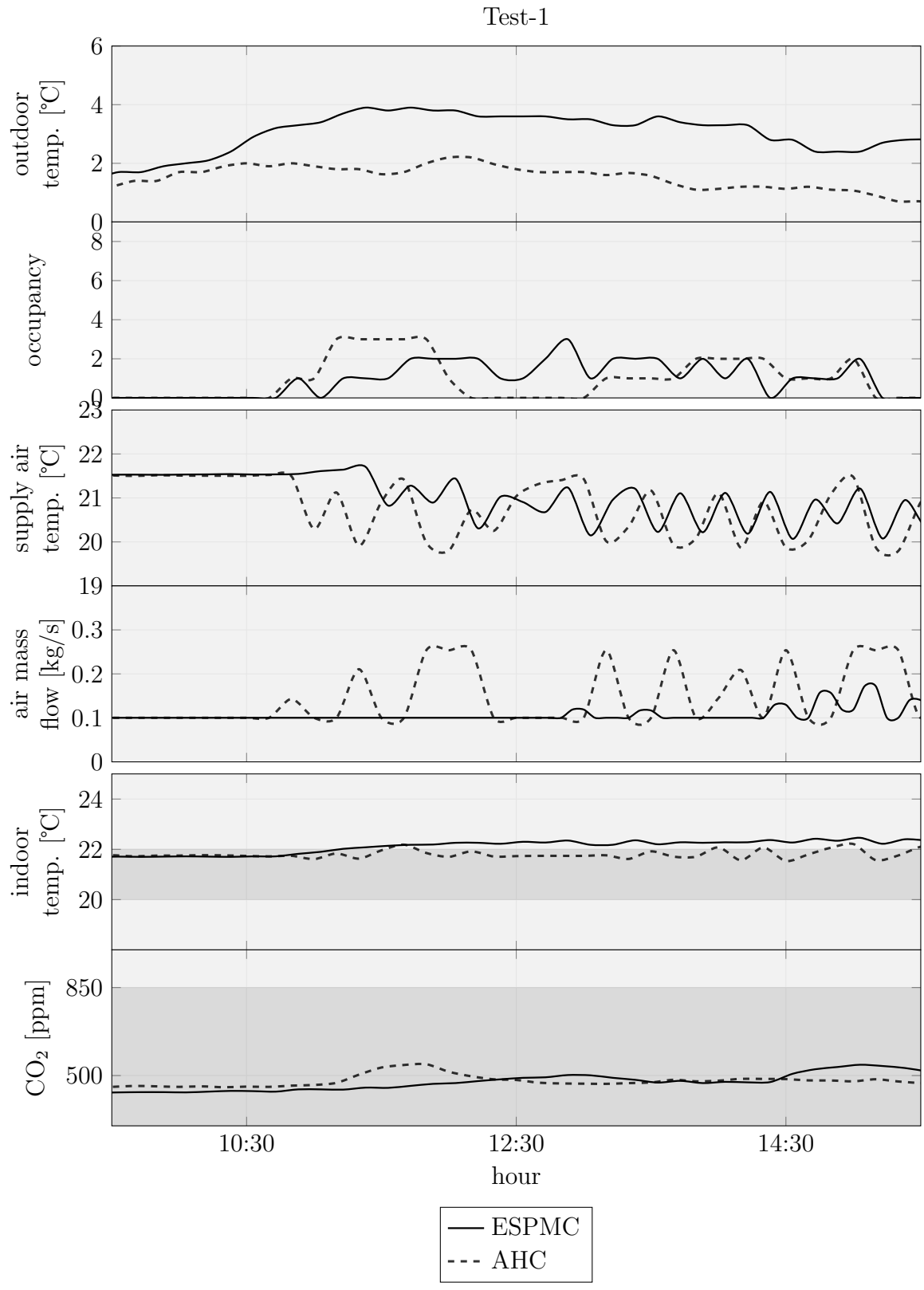

Figure 6.8: Disturbances, CO_2 levels, indoor temperatures and control inputs. The shaded areas represent the comfort bounds.

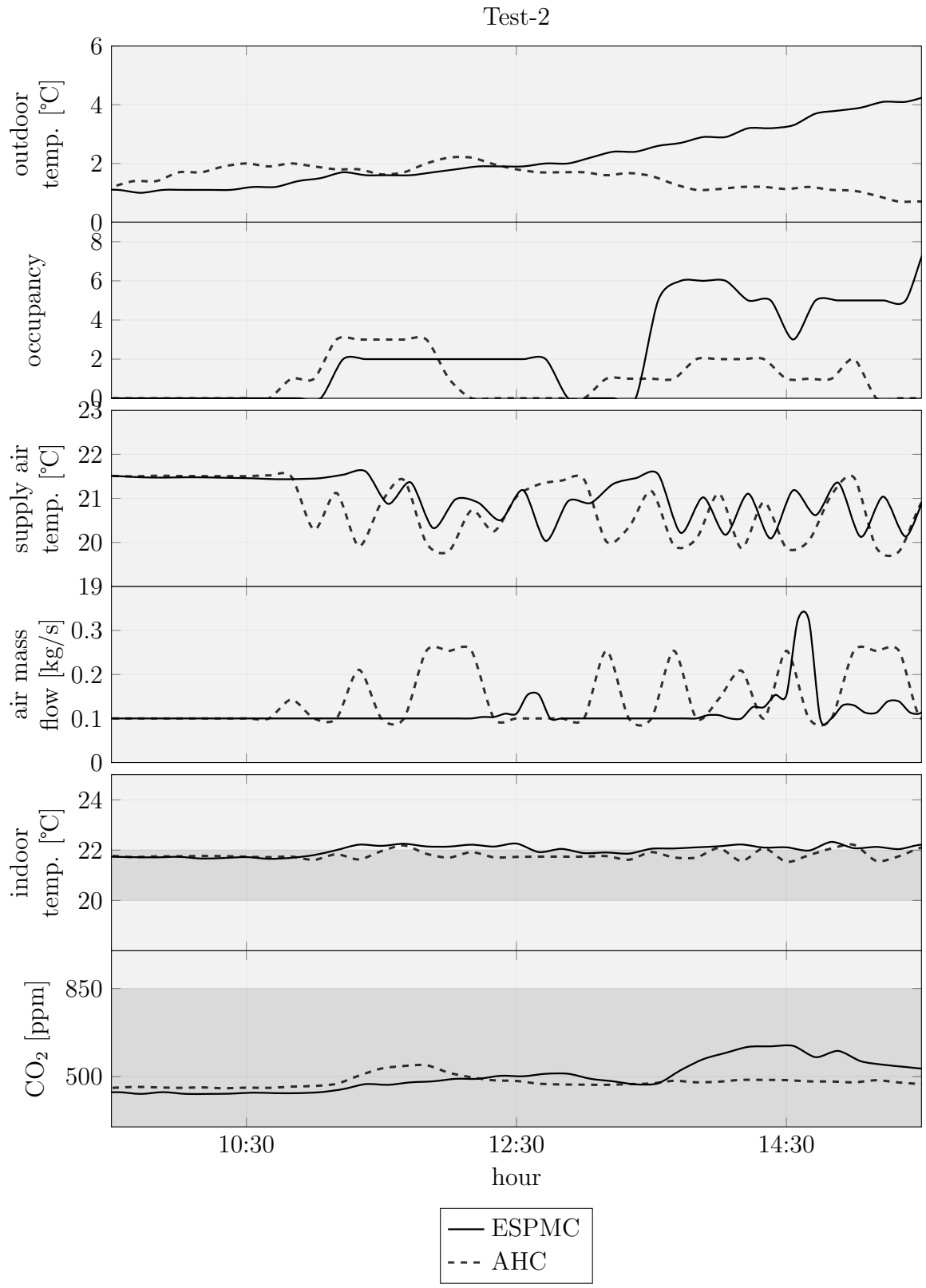

Figure 6.9: Disturbances, CO_2 levels, indoor temperatures and control inputs. The shaded areas represent the comfort bounds.

7 Conclusions

In this thesis several types of MPC controllers for a specific HVAC system have been studied, designed and analyzed.
First of all the simple version of Deterministic MPC has been implemented in an on-line version. To improve the performances of this controller we have then investigated the scenario-based model predictive controller. The differences of the performance between the two approaches emphasize the added value of taking into account, as an uncertain quantity, the disturbances acting on the system. In the simulations it has been shown how the stochastic approach leads to a more robust behaviour with respect to unknown disturbances.
Moreover, in order to reduce the on-line computational time, we have implemented an equivalent stochastic explicit MPC controller. The need to obtain an optimization problem computationally manageable led us to obtain a simplified version for the model of the thermal dynamics. Despite its simplicity, this model had to be able to satisfy the need for accuracy of the predictions not to afflict the effectiveness of the control profile. We experienced how the task to find a model with all these properties can be really hard when it comes to complex thermal dynamic as in our case. Nevertheless the results we have obtained can be considered satisfactory for our proposes. The explicit strategy has been

implemented and tested on a real room of a university building, showing that the resulting actuation laws can be more effective than the current practice. Hence, the main contributions provided in this thesis are : (I) models for the thermal and air quality dynamic of a real test bed; (II)designthe procedures for the implementation of different kinds of Implicit MPC; (III)the analysis of the problem related to the implementation of an off-line predictive controller as, for instance, the computational tractability; (IV) a novel simplified model for the thermal dynamic of the room; (V)the design of a new scheme to run the Explicit MPC on the actual KTH-HVAC system; (VI)a detailed analysis of the behaviour of the aforementioned controller in terms of energy consumption vs. occupancy comfort levels through numerical experiments.

8

Further developments

At the end of this path we are conscious that this field could be rich of possible improvement and possible questions that only a deeper study could show. We present now a list of prospects that came out working on this thesis.

Improving the two state temperature model We observed how the simplified model tends to overestimates the temperature within the room. This fact affects the precision in the prediction that are eventually exploited to obtain the control plan. Thus, improving the thermal model could lead to even more satisfactory results in terms of energy consumption with respect to the implicit approach.

Multi-zone controller It could be interesting to extend the controller we designed to a multi-zone area.

Improve the performance indices There is still the need of measuring precisely and extensively the amount of energy savings/ comfort maintaining performance of the strategy to correctly evaluate the degree of improvements brought to the current practice.

Review the problem of the connection between temperature and CO_2 for explicit MPC The two problems are strictly related and the output of the CO_2 problem represents a lower bound for the temperature model. Since we aim to switch to an off-line computation for the control profile, it is necessary to cluster the possible output of the problem for the air quality. In this thesis a simple heuristic has been proposed but it would be interesting to study deeper this aspect trying to understand whether or not such approximation affects the results of the whole MPC.

Reduce the number of regions The obtained PWA map for the thermal problem has shown a relevant number of regions to consider. This aspect may affect the attractiveness of this method for an implementation on a cheap hardware. A possible development might be to study a way to reduce the number of significant regions with respect to some indices.

Study new types of MPC controller It would be meaningful to develop new MPC controllers which weigh differently the violation of the constraints and hence, to analyze how this affects the performance. Some possibilities might be, for instance, the so-called Integrated Chanche Constraints MPC or the Two-Stage MPC.

Bibliography

[1] a. Boyano, P. Hernandez, and O. Wolf, "Energy demands and potential savings in European office buildings: Case studies based on EnergyPlus simulations," *Energy and Buildings*, vol. 65, pp. 19–28, Oct. 2013.

[2] K. Chua, S. Chou, W. Yang, and J. Yan, "Achieving better energy efficient air conditioning A review of technologies and strategies," *Applied Energy*, vol. 104, pp. 87–104, Apr. 2013.

[3] D. Sturzenegger and D. Gyalistras, "Model Predictive Control of a Swiss office building," *11th REHVA World . . .*, 2013.

[4] A. Barbato, L. Borsani, A. Capone, and S. Melzi, "Home energy saving through a user profiling system based on wireless sensors," *Proceedings of the First ACM Workshop on Embedded Sensing Systems for Energy-Efficiency in Buildings - BuildSys '09*, p. 49, 2009.

[5] Agarwal, "Occupancy-Driven Energy Management for Smart Building Automation."

[6] V. L. Erickson and A. E. Cerpa, "Occupancy based demand response HVAC control strategy," *Proceedings of the 2nd ACM Workshop on Embedded Sensing Systems for Energy-Efficiency in Building - BuildSys '10*, p. 7, 2010.

[7] S. P. Tarzia, R. P. Dick, P. a. Dinda, and G. Memik, "Sonar-based measurement of user presence and attention," *Proceedings of the 11th international conference on Ubiquitous computing - Ubicomp '09*, p. 89, 2009.

[8] K. P. Lam, M. Höynck, B. Dong, B. Andrews, Y.-s. Chiou, D. Benitez, J. Choi, and R. B. Llc, "OCCUPANCY DETECTION THROUGH

AN EXTENSIVE ENVIRONMENTAL SENSOR NETWORK IN AN OPEN-PLAN OFFICE BUILDING Center for Building Performance and Diagnostics , Carnegie Mellon University , Pittsburgh , SENSOR," pp. 1452–1459, 2009.

[9] G. R. Newsham and B. J. Birt, "Building-level occupancy data to improve ARIMA-based electricity use forecasts," *Proceedings of the 2nd ACM Workshop on Embedded Sensing Systems for Energy-Efficiency in Building - BuildSys '10*, p. 13, 2010.

[10] G. Calis, S. Deora, N. Li, B. Becerik-gerber, and B. Krishnamachari, "ASSESSMENT OF WSN AND RFID TECHNOLOGIES FOR REAL-TIME OCCUPANCY INFORMATION," pp. 182–188.

[11] A. Ebadat, G. Bottegal, D. Varagnolo, B. Wahlberg, and K. H. Johansson, "Estimation of building occupancy levels through environmental signals deconvolution," *Proceedings of the 5th ACM Workshop on Embedded Systems For Energy-Efficient Buildings - BuildSys'13*, pp. 1–8, 2013.

[12] J. Scott, A. J. B. Brush, J. Krumm, B. Meyers, M. Hazas, S. Hodges, and N. Villar, "PreHeat : Controlling Home Heating Using Occupancy Prediction," pp. 281–290, 2011.

[13] M. Fadzli Haniff, H. Selamat, R. Yusof, S. Buyamin, and F. Sham Ismail, "Review of HVAC scheduling techniques for buildings towards energy-efficient and cost-effective operations," *Renewable and Sustainable Energy Reviews*, vol. 27, pp. 94–103, Nov. 2013.

[14] W. Grünenfelder and J. Tödtli, "The use of weather predictions and dynamic programming in the control of solar domestic hot water systems," *3rd Mediterranean Electrotechnical Conference*, 1985.

[15] F. Oldewurtel, A. Parisio, C. N. Jones, D. Gyalistras, M. Gwerder, V. Stauch, B. Lehmann, and M. Morari, "Use of model predictive control and weather forecasts for energy efficient building climate control," *Energy and Buildings*, vol. 45, pp. 15–27, Feb. 2012.

[16] L. D. G. Industriel, U. D. Réunion, and A. R. Cassin, "WEATHER SEQUENCES FOR PREDICTING HVAC SYSTEM BEHAVIOUR IN

RESIDENTIAL UNITS LOCATED IN TROPICAL CLIMATES . L . Adelard , F . Garde , F . Pignolet-Tardan , H . Boyer , J . C . Gatina."

[17] M. Gwerder, "Predictive Control for Thermal Storage Management in Buildings," no. October, pp. 1–6, 2005.

[18] A. Bemporad, F. Borrelli, and M. Morari, "Model Predictive Control Based on Linear Programming. The Explicit Solution," pp. 1–23, 2001.

[19] A. Parisio, D. Varagnolo, D. Risberg, G. Pattarello, M. Molinari, and H. Johansson, "Randomized Model Predictive Control for HVAC Systems," 2013.

[20] D. Gyalistras and B. T. Division, *Use of Weather and Occupancy Forecasts For Optimal Building Climate Control (OptiControl): Two Years Progress Report*, 2010, no. September.

[21] F. Borrelli, A. Bemporad, and M. Morari, "for linear and hybrid systems," 2014.

[22] A. Parisio, D. Varagnolo, and M. Molinari, "Implementation of a Scenario-based MPC for HVAC Systems : an Experimental Case Study," 2012.

[23] A. Parisio, M. Molinari, D. Varagnolo, and K. H. Johansson, "A scenario-based predictive control approach to building HVAC management systems," *2013 IEEE International Conference on Automation Science and Engineering (CASE)*, pp. 428–435, Aug. 2013.

[24] G. Calafiore and M. Campi, "The Scenario Approach to Robust Control Design," *IEEE Transactions on Automatic Control*, vol. 51, no. 5, pp. 742–753, May 2006.

[25] J. Drgona, M. Kvasnica, M. Klauco, and M. Fikar, "Explicit Stochastic MPC Approach to Building Temperature Control," *nt.ntnu.no*.